Geomorphology 392 (2021) 107901

Contents lists available at ScienceDirect

Geomorphology

journal homepage: www.elsevier.com/locate/geomorph

Geomorphic history of Lake Manix, Mojave Desert, California: Evolution of a complex terminal lake basin

Marith C. Reheis [a,*], David M. Miller [b], James B. Paces [a], Charles G. Oviatt [c], Joanna R. Redwine [d], Darrell S. Kaufman [e], Jordon Bright [e], Elmira Wan [f]

[a] U.S. Geological Survey, MS-980, Federal Center, Box 25046, Denver, CO 80225, United States of America
[b] U.S. Geological Survey, P.O. Box 158, 350 N. Akron Road, Moffett Field, CA 94035, United States of America
[c] Department of Geology, Kansas State University, 108 Thompson Hall, Manhattan, KS 66506-3201, United States of America
[d] U.S. Bureau of Reclamation, Box 25007, MS 86-68830, Federal Center, Denver, CO 80225, United States of America
[e] School of Earth and Sustainability, Northern Arizona University, Flagstaff, AZ 86011-4099, United States of America
[f] U.S. Geological Survey, 345 Middlefield Rd, MS-975, Menlo Park, CA 94025, United States of America

ARTICLE INFO

Article history:
Received 16 February 2021
Received in revised form 5 August 2021
Accepted 6 August 2021
Available online 13 August 2021

Keywords:
Mojave Desert
Drainage integration
Catastrophic flood
Sedimentation
Tectonics

ABSTRACT

Pluvial lake deposits in the Basin and Range province have long been exploited for records of hydrologic and climatic change. To obtain the most accurate reconstructions, a thorough understanding of the geomorphic evolution of such lake basins must be grounded in field stratigraphy and mapping, which are often lacking or are not well integrated with core studies. We conducted extensive stratigraphic investigation, mapping, and dating of exposed strata in the Lake Manix basin, former terminus of the Mojave River, California, during the Pleistocene to provide such a background and to supplement interpretations from a 45-m-long core.

In this paper, we emphasize the geomorphic and tectonic processes that shaped the evolution of the Manix basin after the arrival of the Mojave River in the early-middle Pleistocene. The main processes include (1) sedimentary infilling of the lake basin, (2) interaction among the subbasins as controlled by internal sills and sill failures, (3) tectonics, and (4) climate change. From about 500 to 190 ka, Lake Manix was confined to its western subbasins, and fluctuated in response to climate change and perhaps to brief diversions of the river into the upstream Harper Lake basin. During this time, about 24 m of sediment accumulated near the confluence of the Mojave River and Manix Wash, and a 15-km-long clastic wedge built into the western basins, gradually filling the accommodation space.

Two basin-integration events subsequently occurred, both caused by failure of sills that lay on sheared deposits along the Manix fault zone. When Lake Manix rose at the onset of glacial marine isotope stage 6, the sill on the south flank of Buwalda Ridge failed and triggered a catastrophic flood that entered the new, lower elevation, previously endorheic Afton subbasin. Subsequent lake-level changes affected both subbasins, but the thickest deposits after the flood are preserved in the Afton subbasin. The area upstream of Buwalda Ridge was only submerged during relatively high lake levels. Thus, sediment records interpreted from the core site and nearby outcrops in part reflect a geomorphic event (basin integration) rather than climatic conditions. The sill of Lake Manix after the integration event lay at the northeast end of the Afton subbasin, athwart strands of the Manix fault zone. At about 25 ka, this eastern sill was rapidly incised, and the river advanced to terminate in Lake Mojave in the Soda and Silver Lake basins. Recognition and dating of integration events, common for lake-river interactions in active tectonic settings, provide important context for interpreting paleoclimate records from sediments and provide temporal and spatial constraints on the biogeography of aquatic species.

1. Introduction

Major progress has been made during the last 40 yr in deciphering the geologic and climatic records of Pleistocene pluvial lakes in the western U.S. using cores from extant lakes (Benson, 2004; Rosenbaum and Reynolds, 2004; Rosenbaum and Kaufman, 2009; Benson et al., 2002, 2011) and from desiccated lakes such as Lake Bonneville (Oviatt et al., 1999), Lakes Searles and Owens (Benson et al., 1996; Bischoff et al., 1997; Smith et al., 1983, 1997), and Lake Manly (Lowenstein et al., 1999; Anderson and Wells, 2003; Forester et al., 2005a). Sedimentology, stable isotopes, pollen and other microfossils, and physical properties from cores provide proxies for changes in lake level, water temperature and chemistry, and ecological conditions in the

* Corresponding author.
E-mail address: mreheis@usgs.gov (M.C. Reheis).

https://doi.org/10.1016/j.geomorph.2021.107901

surrounding landscape. However, such core data do not directly record lake level or reveal many geologic factors that may confound interpretations of proxy data. Moreover, many sediment cores from extant lakes do not extend beyond the last ~40 kyr. In contrast, outcrop studies of incised basin fill (e.g., Oviatt, 1997; Allen and Anderson, 2000; Adams, 2007; Reheis et al., 2002a, 2014a) can provide much longer paleolake histories, indicate absolute lake levels, and yield clues to geologic events such as drainage-basin changes, floods, or earthquakes that can clarify interpretations of sediment and stratigraphy.

The Manix basin in southeastern California is one in a chain of interconnected basins crossed and linked by the modern Mojave River (Fig. 1). The river heads in the San Bernardino Mountains ~100 km to the southwest and in high-water years (Enzel and Wells, 1997) presently flows north and east to its terminus in Silver Lake playa north of Baker, California. During its evolution, the river has integrated several basins that were previously internally drained, including the Victorville, Harper, Hinkley, Manix, and Soda Lake basins (Cox et al., 2003; Enzel et al., 2003; Miller et al., 2020). Sediments in the Manix basin contain a record of Mojave River discharge and lake fluctuations during the middle Pleistocene and most of the late Pleistocene (Jefferson, 2003; Reheis et al., 2012, 2015).

At about 25 cal ka (Reheis and Redwine, 2008; Reheis et al., 2015), Lake Manix overtopped its sill to the northeast and rapidly incised Afton Canyon (Meek, 1989a, 1999) as it drained eastward to form Lake Mojave (Wells et al., 2003; Honke et al., 2019). This event triggered headward erosion through the Manix lake sediments and older basin fill as the Mojave River adjusted to a new, much lower base level, eventually exposing extensive outcrops containing a rich record of lake-level fluctuations, paleoclimate, and geomorphic and geologic events (Jefferson, 2003). We undertook detailed mapping, stratigraphic analysis, and dating of these deposits combined with analysis of water-well records to provide a geologic and geomorphic framework for the basin and to amplify results and interpretations obtained from a 45-m-long core obtained from the central part of the lake basin (Fig. 2). Age control is provided by (1) ^{14}C dating on late Pleistocene deposits (Reheis et al., 2014b, 2015), (2) uranium-series dating on lacustrine tufa and ostracode valves, (3) tephra correlation, (4) correlation using amino acid analysis, and (5) magnetostratigraphy of deposits in the Manix core (Reheis et al., 2012). We use these data to reconstruct the geomorphic history and subbasin sill changes of pluvial Lake Manix and show how those changes are reflected in the paleoclimate record.

2. Climatic, geomorphic, and geologic setting

The Manix basin lies in the central Mojave Desert and is characterized by a warm arid climate. Mean annual temperature in the Barstow area (Fig. 1) is 21.2 °C and annual precipitation is about 125 mm yr^{-1}. Evaporation rates in the Mojave Desert are about 2000 mm yr^{-1} (Blaney, 1957; Enzel, 1992). In contrast, the Mojave River, which fed Lake Manix, has its headwaters on the eastern flank of the San Bernardino Mountains (maximum elevation 3505 m), which receive >1000 mm yr^{-1} of precipitation (wrcc.dri.edu). The development of persistent lakes in the Mojave Desert requires a significant reduction in evaporation rates and at least a doubling of runoff from increased

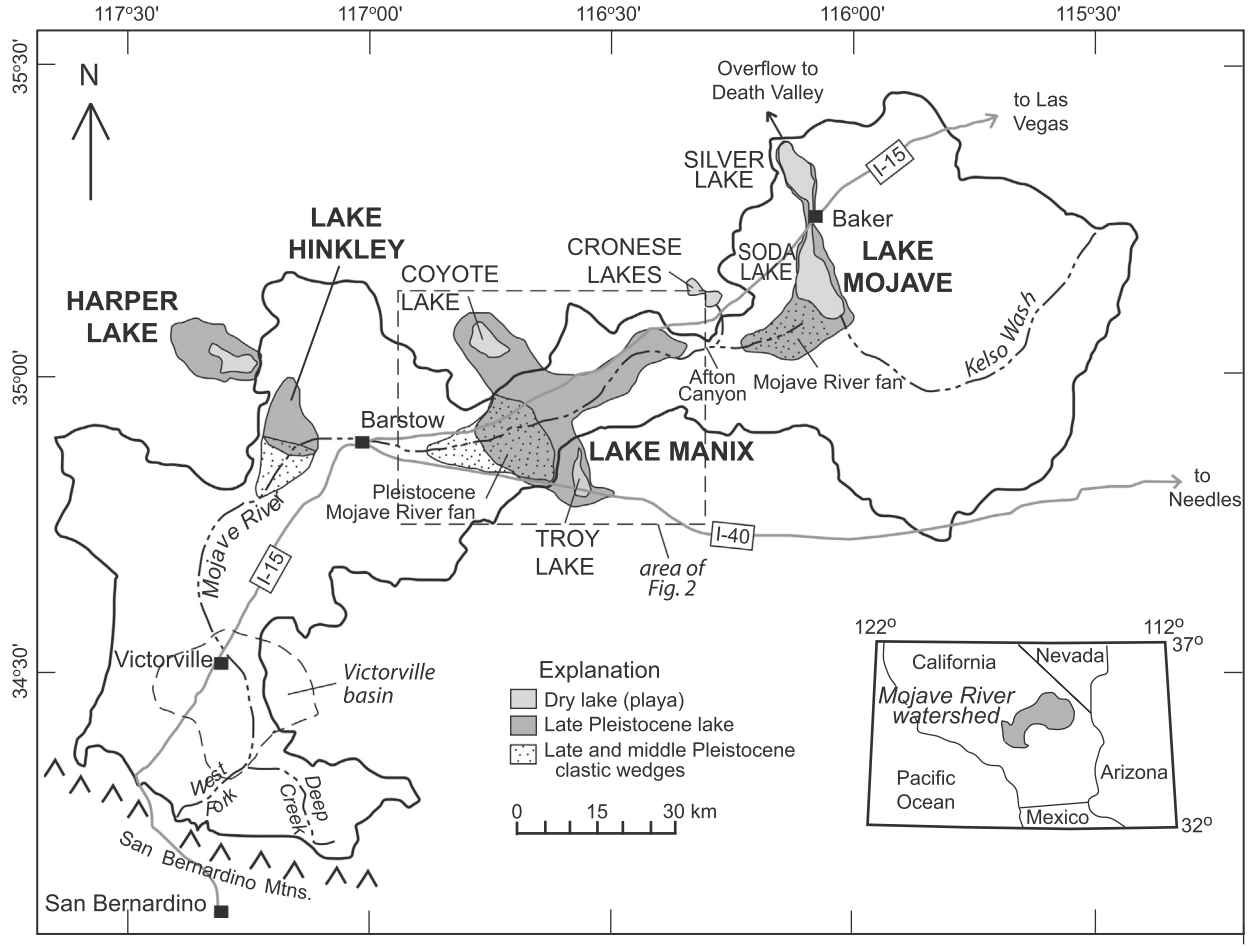

Fig. 1. Map showing lake basins along the Mojave River corridor in southern California (inset). Light gray, extent of modern playa surfaces. Dark gray, extent of late Pleistocene highstands of Harper Lake, Lake Hinkley, Lake Manix, and Lake Mojave.
Modified from Enzel et al. (2003) Reheis and Redwine (2008) and Jefferson (2003).

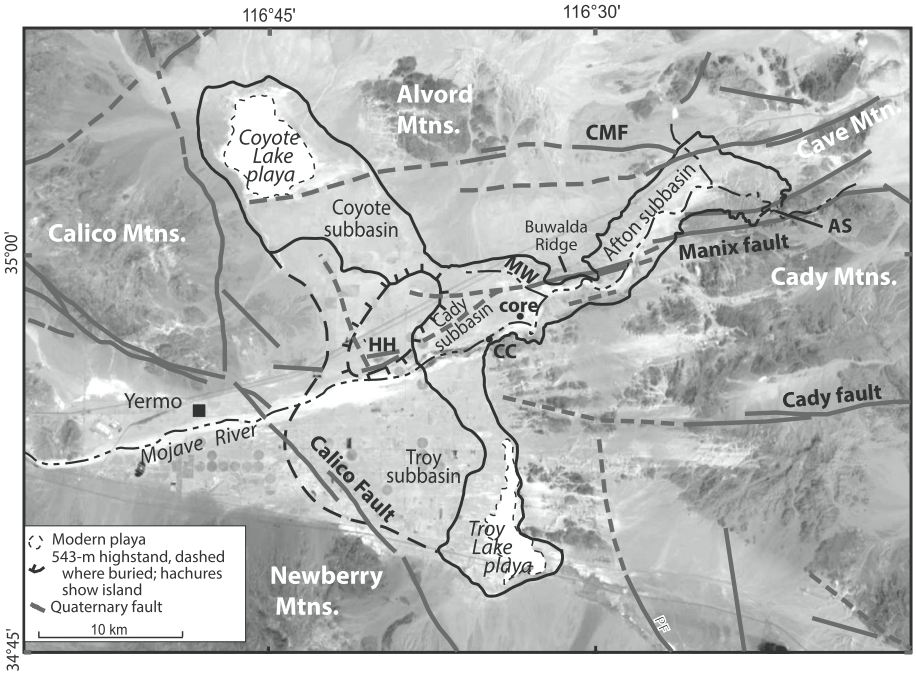

Fig. 2. Orthophoto (U.S. Geological Survey) of the study area. Solid and dashed black lines are important Quaternary faults. AS, Afton sill; CC, Camp Cady; CMF, Cave Mountain fault; HH; Harvard Hill; MW, Manix Wash.
Modified from Figs. 2 and 3 in Reheis et al. (2007) and Miller et al. (2019).

storm frequency in the San Bernardino Mountains (simplified hydrologic model of Wells et al., 2003).

The Manix basin is flanked on the east and south by the Cady Mountains and Newberry Mountains (Fig. 2), a complex of Tertiary volcanic and sedimentary rocks (Danehy and Collier, 1958; Moseley, 1978; Bortugno and Spittler, 1986), with some Mesozoic granitic rocks. Sediments in the Manix basin derived from them, especially alluvial fan deposits, are dominated by mafic volcanic clasts. To the northwest, the Calico Mountains are composed of a wide range of silicic and mafic volcanic and sedimentary rocks (Dibblee Jr., 1968). The Alvord Mountains to the north are composed of Paleozoic schist and marble, granitic Mesozoic rocks, Tertiary volcanic rocks, and younger arkosic sedimentary rocks derived from them (Byers Jr., 1960). These rocks contributed sediment to Pleistocene alluvial fan deposits on the north side of the Mojave River, as well as to the coarse-grained fraction of the early Pleistocene Mojave River formation (informal name; Nagy and Murray, 1991), deposited before the arrival of the Mojave River. Finally, Cave Mountain on the northeast is a massive complex of mafic and felsic Mesozoic plutonic rocks (Danehy and Collier, 1958), and was the source of the fanglomerate of Cave Mountain ("brown fanglomerate" of Ellsworth, 1932), which contains distinctive cobble- to boulder-sized clasts of dark iron-rich rock (Meek, 1989b).

The Manix basin lies within the Eastern California shear zone (Dokka and Travis, 1990). Deformation within this zone has influenced basin geometry over the past 3 million years; the Coyote Lake subbasin has lowered and the Alvord Mountains have risen after deposition of a distinctive Pliocene fluvial unit across their northern margins (Miller and Yount, 2002). This deposit is warped into steep dips adjacent to both the basin and the mountain, suggesting that much of today's topography is youthful. The Mojave River formation is significantly deformed adjacent to the Manix fault (McGill et al., 1988; Reheis et al., 2014b). The Calico, Dolores Lake, Cave Mountain, and Manix faults displace Pleistocene and older sediments (Fig. 2), and most faults have strong evidence for Holocene rupture. Sheared zones in fanglomerate units along the Manix fault zone have played a significant role in the drainage integration history as this fault zone coincides with the former northeastern sill of Lake Manix and with the boundary between the Cady and Afton subbasins.

The Manix basin is composed of several subbasins: the southern Troy Lake subbasin, the central Cady subbasin (previously referred to as the Manix subbasin), the northern Coyote Lake subbasin, and the northeastern Afton subbasin (Fig. 2). A fifth area that may represent another subbasin lies west of the town of Yermo. West of the Cady Mountains, water-well logs indicate that there was at most a subtle divide between the Cady and Troy Lake subbasins during the deposition of Lake Manix sediment. The Troy Lake area was almost filled by fluvial deposits of the Mojave River during and after the late Pleistocene phase of Lake Manix (Groat, 1967; Reynolds and Reynolds, 1985; Meek, 1990) and has not been much incised. In contrast, the Cady and Coyote Lake subbasins are separated by low hills of Tertiary rocks and are connected by a bedrock-controlled sill (~540 masl) over which water was transferred between the subbasins during high lake levels of the late Pleistocene (Meek, 1990). Fluvial terraces west of Harvard Hill and dated lacustrine deposits indicate that occasionally the Mojave River fed the Coyote Lake subbasin directly during the latest Pleistocene (Meek, 1994, 2004; Miller et al., 2019). The Cady and Afton subbasins presently are not separated by a divide, but the sedimentary sequences preserved within them indicate that the subbasins were separate in the past, as discussed below. The boundary between them is defined by Buwalda Ridge (Fig. 2), which is composed of Pliocene fanglomerate bounded on the south and internally cut by strands of the Manix fault.

2.1. Previous work

Deposits of Pleistocene Lake Manix (the Manix Formation of Jefferson, 1968) have been studied for over a century. The lake beds were first named and associated vertebrate fossils identified by Buwalda (1914), for whom Buwalda Ridge is now named (Fig. 2). The stratigraphy, paleontology, and broad lake-level fluctuations were established by Ellsworth (1932), Blackwelder and Ellsworth (1936), Jefferson (2003, and references therein), and Meek (1989a, 1989b, 1999, 2000). Enzel et al. (2003) reviewed some of this literature, and Reheis and Redwine (2008) and Reheis et al. (2015) addressed the late Pleistocene record of lake levels, overflow, and eventual incision of Afton Canyon. Miller et al. (2019) reconstructed the late Pleistocene

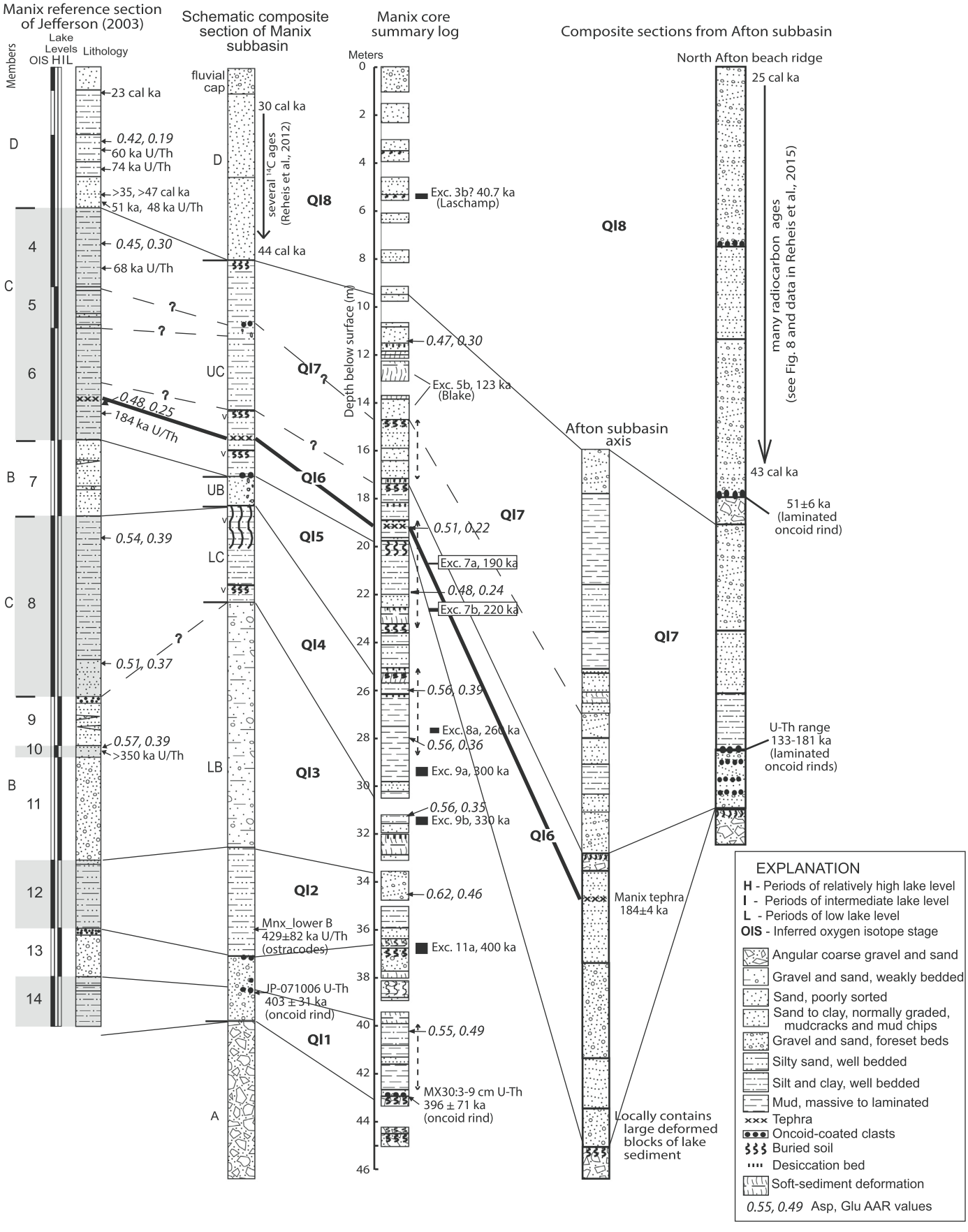
Manix reference section of Jefferson (2003)
Lake Levels
OIS HIL
Lithology
Members
23 cal ka
0.42, 0.19
60 ka U/Th
74 ka U/Th
>35, >47 cal ka
51 ka, 48 ka U/Th
0.45, 0.30
68 ka U/Th
0.48, 0.25
184 ka U/Th
0.54, 0.39
0.51, 0.37
0.57, 0.39
>350 ka U/Th
Schematic composite section of Manix subbasin
fluvial cap
30 cal ka
several 14C ages (Reheis et al., 2012)
44 cal ka
UC
UB
LC
LB
A
Qf8
Qf7
Qf6
Qf5
Qf4
Qf3
Qf2
Qf1
Mnx_lower B 429±82 ka U/Th (ostracodes)
JP-071006 U-Th 403 ± 31 ka (oncoid rind)
Manix core summary log
Meters
Depth below surface (m)
Exc. 3b? 40.7 ka (Laschamp)
0.47, 0.30
Exc. 5b, 123 ka (Blake)
0.51, 0.22
Exc. 7a, 190 ka
0.48, 0.24
Exc. 7b, 220 ka
0.56, 0.39
Exc. 8a, 260 ka
0.56, 0.36
Exc. 9a, 300 ka
0.56, 0.35
Exc. 9b, 330 ka
0.62, 0.46
Exc. 11a, 400 ka
0.55, 0.49
MX30:3-9 cm U-Th 396 ± 71 ka (oncoid rind)
Composite sections from Afton subbasin
Afton subbasin axis
Manix tephra 184±4 ka
Locally contains large deformed blocks of lake sediment
North Afton beach ridge
25 cal ka
many radiocarbon ages (see Fig. 8 and data in Reheis et al., 2015)
43 cal ka
51±6 ka (laminated oncoid rind)
U-Th range 133-181 ka (laminated oncoid rinds)
EXPLANATION
H - Periods of relatively high lake level
I - Periods of intermediate lake level
L - Periods of low lake level
OIS - Inferred oxygen isotope stage
Angular coarse gravel and sand
Gravel and sand, weakly bedded
Sand, poorly sorted
Sand to clay, normally graded, mudcracks and mud chips
Gravel and sand, foreset beds
Silty sand, well bedded
Silt and clay, well bedded
Mud, massive to laminated
Tephra
Oncoid-coated clasts
Buried soil
Desiccation bed
Soft-sediment deformation
0.55, 0.49 Asp, Glu AAR values

diversion of the Mojave River into Coyote subbasin and its subsequent highstands after the demise of Lake Manix and demonstrated that previous diversions occurred during the time of Lake Manix. Here, we summarize research pertinent to the lake-bed stratigraphy. All previous workers interpreted the stratigraphic sequence in the Afton subbasin to represent two main lake phases, although Meek (1990) suggested there were older lake deposits. The younger lake is mainly represented by nearshore sand and gravel, and the older lake by generally deeper-water deposits. Meek (1989a, 1990, 1999, 2000, 2004) dated beach deposits of the younger lake phase in the Afton, Coyote Lake, and Troy Lake subbasins.

Jefferson (1968, 1985, 2003) studied the stratigraphic sequence exposed near the confluence of the Mojave River and Manix Wash and concluded that the Manix Formation there recorded five deep-lake cycles proposed to correlate with marine-isotope stages (MIS) 4, 6, 8, 12, and 14 (Fig. 3), spanning 57–563 ka (Lisiecki and Raymo, 2005). The correlations of sediments older than MIS 6 (>191 ka) were constrained by a single U—Th age of >350 ka on bone (Jefferson, 2003). Deposits interpreted as perennial-lake sediments and correlated with MIS 6 contain a tephra layer near the base that had an assigned age of 185 ka based on chemical correlation with a rhyolite in the southern Sierra Nevada; this tephra (henceforth referred to as the Manix tephra) was also associated with a uranium-series age on bone of about 184 ka (Jefferson, 2003). Reheis et al. (2012) obtained a ^{40}Ar—^{39}Ar sanidine age of 184 ± 4 ka on the source rhyolite. Sediments representing a sequence of fluctuating lake levels were correlated with MIS 4 based on several uranium-series ages on bone ranging from 68 to 48 ka and three radiocarbon ages (two were infinite; Jefferson, 2003, p. 48). Reheis et al. (2012) published six ^{14}C ages for these uppermost sandy sediments (Fig. 3), ranging from 44.0 cal ka to 30.4 cal ka.

Reheis and Redwine (2008) revised the late Pleistocene history of Lake Manix and the record of downstream integration by the Mojave River using stratigraphy, radiocarbon ages, and soils. They showed that Lake Manix reached a highstand of 547–558 masl (meters above sea level) at least twice prior to its previously known 543-m highstands; soil properties indicated an age of at least 35–50 ka. Beach deposits, locally with preserved barrier morphology, document the older highstands in both the Afton and Cady subbasins. During one or more of these older highstands, the lake spilled east over a sill on the north rim of Afton Canyon to the Soda Lake basin (Lake Mojave; Fig. 1). However, significant incision of the canyon did not begin until about 25 cal ka, consistent with interpretations of Wells et al. (2003) and Honke et al. (2019) that episodic flooding of the downstream Lake Mojave basin may have begun as early as 26.5 cal ka.

This paper provides new information on (1) the western subbasins of Lake Manix derived from interpretation of water-well logs, (2) uranium-series ages on oncoidal tufa, ostracodes, and root casts, and (3) stratigraphic and sedimentologic descriptions that illuminate the pre-MIS 6 record based on surficial geologic mapping (Reheis et al., 2014b). We combine this new information with previously published data and interpretations on (4) the incision of Afton Canyon (Reheis and Redwine, 2008), (5) the climate record of Lake Manix and a subbasin-integration event from a 45-m-long core and outcrop evidence (Reheis et al., 2012), (6) a detailed lake-level record for MIS 3 from outcrops and radiocarbon dating (Reheis et al., 2015), and (7) the paleoclimate record of Lake Coyote (Miller et al., 2019) to synthesize a complete geomorphic history of Lake Manix for the past half-million years. Readers are referred to Reheis et al. (2015) for information on all calibrated ^{14}C ages cited in the present paper.

3. Methods

We conducted comprehensive surficial-deposits mapping of the deposits along the course of the modern Mojave River to unravel the history of river, lake, and fault interactions (Reheis et al., 2014b). Positions of study sites used in this paper (Table 1) were recorded using either a handheld GPS or, for precise control, a high-precision instrument to obtain differentially corrected elevations with vertical errors of about ±50–100 cm. Stratigraphic sections were described at numerous locations. *Anodonta californiensis* (freshwater clam) shells and ostracode-bearing sediments, suitable for radiocarbon dating, amino acid analysis, and interpretation of hydrologic environments, were collected from outcrop exposures. Tephra layers provided correlated radiometric ages for some strata (Reheis et al., 2014b). Radiocarbon analyses and techniques are reported in Reheis and Redwine (2008) and Reheis et al. (2015) and the results are briefly summarized here. Samples of lake tufa, termed "oncoids" by Awramik et al. (2000), nodules, rhizoliths, and ostracode valves were obtained for uranium-series dating. Oncoid coats typically formed as stromatolitic carbonate coats and are reliable indicators of lake transgressions in the Manix basin (Reheis and Miller, 2010).

3.1. Tephra analysis

Stratigraphic sections within the study area locally contain tephra layers, most of which are contained within the Mojave River formation and older fanglomerates (Reheis et al., 2014b). The U.S. Geological Survey Tephrochronology Laboratory has identified these through chemical correlation with tephra samples of known age. Glass shards from tephra layers were analyzed by electron microprobe for major-oxide composition using methods described by Sarna-Wojcicki et al. (1984). Sample compositions were compared with compositions in a database of previously analyzed tephra layers using statistical programs. Correlations were based on similarity in chemical composition, petrographic characteristics (such as shard morphology and phenocryst mineralogy), and stratigraphic data. Here, we use mainly the age of the 184-ka Manix tephra (analytical data reported in Reheis et al., 2012), which is important to the age and correlation of lake units and events.

3.2. Uranium-series dating

Lacustrine tufa has been dated in pluvial lake basins of Nevada and California (e.g., Kaufman and Broecker, 1965; Ku et al., 1998; Lao and Benson, 1988; Kurth et al., 2011). However, these materials present challenges for U-series dating because of the possibilities of initial ^{230}Th, post-depositional losses and gains of U from groundwater and precipitation of younger calcite in pore spaces.

Most samples in this study consisted of carbon ate coatings that contain lobate structures with concentric growth layering like fabrics observed in stromatolites. Our study indicates that crusts may not have formed entirely while their substrates were exposed at the water/sediment interface. Samples are commonly free of visible detritus under binocular magnification. However, examination of thin sections with a petrographic microscope suggests that some samples were affected by post-depositional processes such as replacement of primary calcite or growth by displacement of surrounding sediment (e.g., Goudie, 1983; Reheis et al., 1992). Most analyses of the crusts have elevated concentrations of common Th (^{232}Th), indicative of finely dispersed clays or silts that cannot be separated by mechanical means. Small subsamples

Fig. 3. Composite measured sections comparing, from left to right: (1) reference section for the Manix Formation near the confluence of Manix Wash and the Mojave River in Cady subbasin, showing age control, map units, and correlations to marine oxygen-isotope stages (Jefferson, 2003); (2) composite section measured in the same area (Oviatt et al., 2007) with U—Th age from this study (Table 2); (3) summary sediment log for the Manix core, showing age control provided by magnetic excursions (Exc.; Reheis et al., 2012) and conflicting U—Th age; and (4) composite sections from the Afton subbasin showing age control provided by radiocarbon, U-series, and tephra correlations (Reheis et al., 2014b). Note positions of intervals showing possible earthquake-induced features and bold black line marking the Manix tephra in the core. Also shown are amino acid racemization values (AAR) for aspartic acid and glutamic acids measured in ostracodes from outcrop and core samples.

Table 1
Locations of measured sections and other study sites in Manix basin used in this paper.

Station	Latitude, Longitude (degrees, WGS84)	Description	See figure or table
M04-29B	35.0653 −116.4380	Section in Ql8, upper Dunn wash; point is top of beach ridge	Figs. 7 and 8
M04-75	34.9818 −116.5359	Section on S side of Buwalda Ridge; point is base of Ql7	Figs. 4 and 5
M05-19	35.0630 −116.4339	Section in upper Dunn wash; point is base of Ql7	Figs. 7 and 8
M05-25	35.0447 −116.3656	U-series age on ostracodes in Ql7 on E side of North Afton beach ridge (see Reheis et al., 2014b for measured section).	Fig. 7; Table 2
M05-26	35.0435 −116.3695	Section on W side of North Afton beach ridge; point is base of Ql7	Figs. 7 and 8
M05-52E	35.0580 −116.4287	Section in lower Dunn wash; point is base of Ql8	Figs. 7 and 8
M05-54	35.0490 −116.4250	Section in railroad cut in Ql6, W side of lower Dunn wash; U-series age on rhizoliths	Figs. 7, 8 and 9; Table 2
M05-58-60	35.0301 −116.4528	Section SW of Dunn siding; point is base of Qto	Figs. 7 and 9
M05-61	35.0426 −116.3927	Section on N side of Mojave River, E of Dunn wash; point is base of Ql6	Figs. 7 and 8
M05-65	35.0456 −116.3731	Section on W side of North Afton beach ridge; point is base of Ql6	Figs. 7, 8 and 9
M06-04	35.0457 −116.4243	Section near mouth of Dunn wash; point is base of Ql6	Figs. 7, 8 and 9
M06-28	35.0430 −116.3764	Point on base of Ql6, west of North Afton beach ridge	Figs. 7 and 9
M06-62B	35.0295 −116.3864	U-series age on tufa at base of Ql8, S side of Mojave River. Sample projected into section J06D-206 on Fig. 8	Fig. 7; Table 2
M06-70	35.0302 −116.4361	Section S of Dunn siding; point is top of Qto	Figs. 7 and 9
M06-77	35.0298 −116.4495	Section SW of Dunn siding; point is base of Qto	Figs. 7, 8 and 9
M06-81	35.0170 −116.4747	Section NE of Buwalda Ridge; point is base of Ql7	Figs. 7 and 8
M06-91	34.9852 −116.4980	Section on S side of Buwalda Ridge; point is base of Ql7	Figs. 7 and 8
M06-100	35.0369 −116.4336	Section on N side of Mojave River, SSE of Dunn siding; point is base of Qto	Figs. 6, 7, 8 and 9
M06-119	35.0467 −116.3716	Highest Ql6 in Afton subbasin, W side of North Afton beach ridge	Figs. 7 and 9
M06-142	35.0447 −116.3623	Section east of North Afton beach ridge; point is base of Ql8	Figs. 7 and 8
M06-145	35.0403 −116.3554	U-series age on tufa at base of Ql7, east of North Afton beach ridge	Fig. 7; Table 2
M06-156	35.0370 −116.3524	Section east of North Afton beach ridge; point is top of Ql7	Figs. 7 and 8
M06-166	35.0561 −116.4001	Point on base of Ql6 east of Dunn wash	Figs. 7 and 9
M07-41	35.0234 −116.4678	Photo of deformed beds of Ql7	Fig. 11A
M07-62	35.0302 −116.4627	Section exposed in railroad cut; point is base of section	Figs. 7 and 8
M07-66	35.0110 −116.4987	Section N of Buwalda Ridge; point is base of Ql7	Figs. 7 and 8
M07-78A	34.9924 −116.5061	Ql7 beach ridge crest, 554 masl, N flank of Buwalda Ridge	Fig. 7
M07-117	34.9868 −116.4881	Section in Qto and Ql7 deposits on S flank of Buwalda Ridge	Figs. 7, 8 and 9
M07-138	34.9891 −116.4555	Ql7 beach gravel, 553 masl, E of Buwalda Ridge, S side of Mojave River	Fig. 7
M07-144	34.9983 −116.4692	Section in Qto exposed in river bluffs E of Buwalda Ridge	Figs. 7 and 9
M07-159	35.0554 −116.4214	Section near Dunn wash containing Manix tephra; point is base of Ql6	Figs. 7, 8 and 9
M08-02	35.0342 −116.4482	Photos of deformed beds in Ql7, west of DI section	Figs. 7 and 11
M08-45	35.0054 −116.4658	Section NE of Buwalda Ridge exposed in river bluffs; point is base of Qto	Figs. 7, 8 and 9
M08-60	34.9824 −116.5476	Section on E side of Manix Wash; point is base of Ql8	Figs. 4, 5 and 9
M08-110	34.9870 −116.5581	Section in bluffs of Manix Wash; point is top of section	Figs. 4 and 5
M09-05	34.9878 −116.5550	Section on E side of Manix Wash; point is base of Ql7	Figs. 4 and 5
M09-06	35.0225 −116.4795	Section in Ql8, NE of Buwalda Ridge exposed in railroad cut	Figs. 7 and 8
M09-29	34.9609 −116.5396	Section south of Manix Wash on S side of river; point is base of Ql4	Figs. 4 and 5
M09-32	34.9600 −116.5543	Photo of sand blow exposed in bluffs near Manix Wash	Figs. 4 and 11E
M09-58	34.9560 −116.5379	Section south of Manix Wash on S side of river; point is base of Ql6	Figs. 4, 5, 6A and 9
M09-76	34.9642 −116.5165	Section SE of Manix Wash on S side of river; point is base of Ql6	Figs. 4, 5 and 9
M09-127	34.9864 −116.4882	Section on S flank of Buwalda Ridge; point is base of Qto flood deposits	Figs. 7, 8 and 9
M10-11	34.9720 −116.5545	Section W of Manix Wash on S side of river; point is base of Ql6	Figs. 4 and 9
M10-59	34.9816 −116.5305	Section on S flank of Buwalda Ridge; point is base of Ql6, highest in Cady subbasin	Figs. 4, 5 and 9
DI-1	35.0362 −116.4416	Section SW of Dunn siding; point is base of Ql7	Figs. 7 and 8
JR06D-202	35.0322 −116.3942	U-series ages on tufa at base of Ql7, S side of Mojave River	Fig. 7; Table 2
JR06D-206	35.0268 −116.3960	Section on S side of Mojave River; point is top of Ql8	Figs. 7 and 8
JO-7	34.9739 −116.5562	Section S of Manix Wash on N side of river; point is base of Ql6	Figs. 4 and 5
JO-13	34.9706 −116.55174	Section S of Manix Wash on N side of river; point is base of Ql6	Figs. 4, 5 and 9
JO-14	34.9662 −116.5531	Section S of Manix Wash on N side of river; point is base of Ql6	Figs. 4, 5 and 6C

(median weight of 38 mg) targeted the most detritus-free, dense layers, which are least likely to be affected by detrital contamination or secondary U mobility (see Appendix A and Paces and Reheis, 2021, for sample details). Because of the possibility of post-depositional modification and the presence of detrital Th, U-series ages determined on oncoids should be used with caution.

U-series data were determined at U.S. Geological Survey radiogenic isotope laboratories in Denver, Colorado, by isotope-dilution, thermal-ionization mass spectrometry (ID-TIMS). Detailed analytical protocols are described in Appendix A (data are in Paces and Reheis, 2021). Subsamples spiked with known quantities of ^{236}U, ^{233}U, and ^{229}Th were totally dissolved using nitric and hydrofluoric acids to avoid laboratory fractionation of U and Th (Bischoff and Fitzpatrick, 1991), purified by anion exchange, and analyzed on a Thermo Finnigan Triton™ TIMS using a single discrete-dynode electron multiplier operating in peak jumping mode. Measured atomic ratios were converted to [$^{232}Th/^{238}U$], [$^{230}Th/^{238}U$], and [$^{234}U/^{238}U$] (square brackets used to denote activity ratios) using accepted values for radioactive decay constants (Steiger and Jäger, 1977; Cheng et al., 2013).

$^{230}Th/U$ ages and initial [$^{234}U/^{238}U$] values were calculated for the isotopic compositions of "pure" authigenic carbonate cements, obtained either by subtracting an assumed detrital component or by using a 3-dimensional isochron approach that does not require assumptions about detrital compositions (Ludwig and Paces, 2002). The effects of secondary U mobility were assessed by evaluating how closely initial [$^{234}U/^{238}U$] values matched those expected for paleo-Lake Manix surface water (Fig. S4 in Appendix A). The resulting [$^{234}U/^{238}U$] estimate (1.39 ± 0.06) was used to calculate model $^{234}U/^{238}U$ ages for those suspect samples. Methods used to produce best-age estimates for each sample are described in Appendix A (also Paces and Reheis, 2021).

3.3. Ostracode faunal analysis

To obtain fossil ostracodes, sediment samples were processed using the microfossil protocol developed for the U.S. Geological Survey in Denver, Colorado (Forester, 1988), except that a weak sodium bicarbonate and sodium hexametaphosphate aqueous solution was used as a deflocculant instead of Calgon®. Ostracodes were identified to species

whenever possible using Delorme (1967, 1971), Forester (1985), and Steinmetz (1988). The amino acid analyses and U-series dating presented in this study were performed on valves that were identified to species. For a few outcrop samples from Afton subbasin that were not reported in Reheis et al. (2012), relative abundances were estimated rather than counted.

3.4. Amino-acid analysis

Ostracode valves were prepared for amino acid racemization (AAR) analysis according to methods described by Kaufman (2003) and analyzed by using reverse-phase high-performance liquid chromatography (HPLC; Kaufman and Manley, 1998). We focused on aspartic acid (Asp) and glutamic acid (Glu) because these two amino acids are especially abundant in ostracode protein and are well-resolved chromatographically. We analyzed 21 samples of mono-specific ostracode valves for AAR: 20 samples composed the most common ostracode in the Manix area, *Limnocythere ceriotuberosa*, and one sample composed *Limnocythere platyforma*. Each sample comprised an average of 12 independently analyzed subsamples, each of which comprised two or three valves, for a total of 233 subsamples. Thirty-seven individual subsamples (16% overall) yielded D/L (right-handed/left-handed) values that were excluded based on criteria outlined in Kosnik and Kaufman (2008). The remaining results were then averaged to yield a single D/L value for each sample. The rate of AAR increases with increased temperature and varies for different amino acids and taxonomy (Wehmiller and Miller, 2000). Rates of AAR in the Manix area are likely to be much higher compared to areas farther north where racemization rates in ostracode valves have been previously determined, such as the Bonneville basin (Oviatt et al., 1999; Kaufman, 2003), and might be strongly affected by length of exposure in outcrop. Thus, we use D/L values for ostracodes from age-constrained intervals of the Manix core (unaffected by outcrop exposure) to correlate between the core and other sample sites.

3.5. Water well analysis

Several thousand water wells have been drilled across the Mojave River plain and adjacent areas for agricultural and domestic uses. We selected about ¾ of these for potential study based on location, and of these, about 750 had well logs that conveyed information useful for understanding the Manix lake system and its overlap deposits. Each log was examined for lithologic intervals and boundaries that may be correlatable within the basin, such as blue or green clay, coarse gravel, cementation, and depth to pre-Manix deposits. Wells were selected in broad transects parallel to the Mojave River and in areas with known Quaternary faulting, as well as areas with sparse well coverage throughout the basin. The well information was summarized in a spreadsheet, imported into GIS, and subjected to spatial analysis.

4. Subbasins of Lake Manix

Prior to the arrival of the Mojave River from upstream, the Manix basin area was occupied by several separate endorheic basins: the Coyote Lake, Yermo, Cady, Troy, and Afton basins (Fig. 2); all but Yermo were floored by playas and surrounded by fringing alluvial fans. During the history of Lake Manix, the larger subbasins of Coyote Lake, Cady-Troy, and Afton were separated at various times by sills that influenced the depositional sequences within them and the degree of dissection by the Mojave River.

Because exposures of deposits of Lake Manix in the area west of Manix Wash are scarce, we relied largely on water well analysis for the western part of the lake. Much of the area from southern Coyote Lake basin southward to the west side of Troy Lake and west to Daggett is covered by fluvial plain deposits 3–10 m thick (unit Qt, Fig. 4). These deposits postdate the draining of Lake Manix and are characterized by lenticular fluvial sand and gravel deposits with subdued ridge-and-valley topography in which the ridges are capped by gravels, topography evidently having formed by inversion driven by deflation (Hagar, 1966; Meek, 1994; Miller et al., 2019). Beneath the fluvial plain deposits are fluvial delta deposits traceable in the banks of the Mojave River channel westward to Yermo. These deltaic deposits represent the youngest transgressive cycles of the lake, which was constrained to eastern basins. The lacustrine deposits beneath the deltaic deposits are traceable from Manix Wash westward to near Camp Cady, where lacustrine fines are present in the bed of the Mojave River. Tectonically uplifted blocks at Harvard Hill and Toomey hill (Fig. 4; 34.932°N, 116.725°W) expose small patches of lacustrine fines, sand, gravel, and wetland deposits. Water-well records provide a larger, if imprecise, view of the underlying lacustrine and fluvial deposits of the western subbasins of Lake Manix.

4.1. Water well stratigraphy: Yermo, Troy, Cady subbasins

4.1.1. Proximal clastic wedge

Carefully logged wells west of Yermo (Fig. 4; Densmore et al., 1996) demonstrate that the fluvial plain sediment is 6 to 12 m thick and lies on extremely thick gravel and sand deposited by the Mojave River. Thicknesses of this clastic section range from 100 to 180 m. The gravel lies on older, possibly Tertiary, rocks. Although Densmore et al. (1996) indicated a break in age within the Mojave River gravel section, the geophysical logs do not support a large break and no indicators of soils or other evidence for a major break are reported in the sediment logs. For simplicity we treat this section as a single, long-duration clastic wedge accumulation that formed at the mouth of the newly developed confined river channel immediately upstream of Daggett.

About 4 km east of Daggett, the clastic wedge changes to gravel intertonguing with sand, first as three major cycles and farther east as five to seven cycles of deposition. The gravels extend east of the Calico fault a few kilometers to about 15 km from Daggett. Sand wedges within the eastern part of the clastic wedge change to fine sand and silt about 9 km east of the apex of the clastic wedge, and reduced fines (blue clay in driller logs) appear within the fines about 11 km east of the apex. Thus, the clastic deposits intertongue with lake and lake-margin (beach and nearshore sands) deposits through much of their extent. Overall, the clastic wedge extends nearly halfway across the basin and occupies a significant fraction of the volume in the basin.

The base of the clastic wedge near Daggett is below highstand levels of Lake Manix, indicating that the Mojave River debouched into a basin that filled with water and gravel synchronously. Evidence for an eastward-rising base of the clastic wedge toward Yermo may indicate that the earliest deposits of the wedge filled a local pre-Manix basin 3–5 km wide before prograding farther eastward (Fig. 4). The well records in this area do not include lacustrine deposits, indicating that the wedge aggraded more rapidly than water levels rose during early lake history. The youngest of the sand tongues within the wedge is higher in elevation than the highstands of Lake Manix. It may represent a deltaic facies, a beach facies associated with the 558 m lake shoreline, or it may have been uplifted by the Calico fault or by folding. Well records are inadequate for distinguishing between delta and beach sediment and for distinguishing tectonic movements less than ~20 m.

4.1.2. Base and thickness of the lake deposits

The base of lake deposits is generally evident in the well logs as a change from sand, silt, and clay downward to coarse rocky gravel, cemented deposits, and bedrock. Interpretation of a few well logs are complicated by underlying sediments that also are lacustrine. The most prominent example of this is north of the Manix fault, where the Miocene Barstow Formation siltstone, shale, limestone, and sandstone crop out in every hill that rises above the fluvial plain and also occur at depth. A basalt flow in one area north of Harvard Hill (HH, Fig. 4)

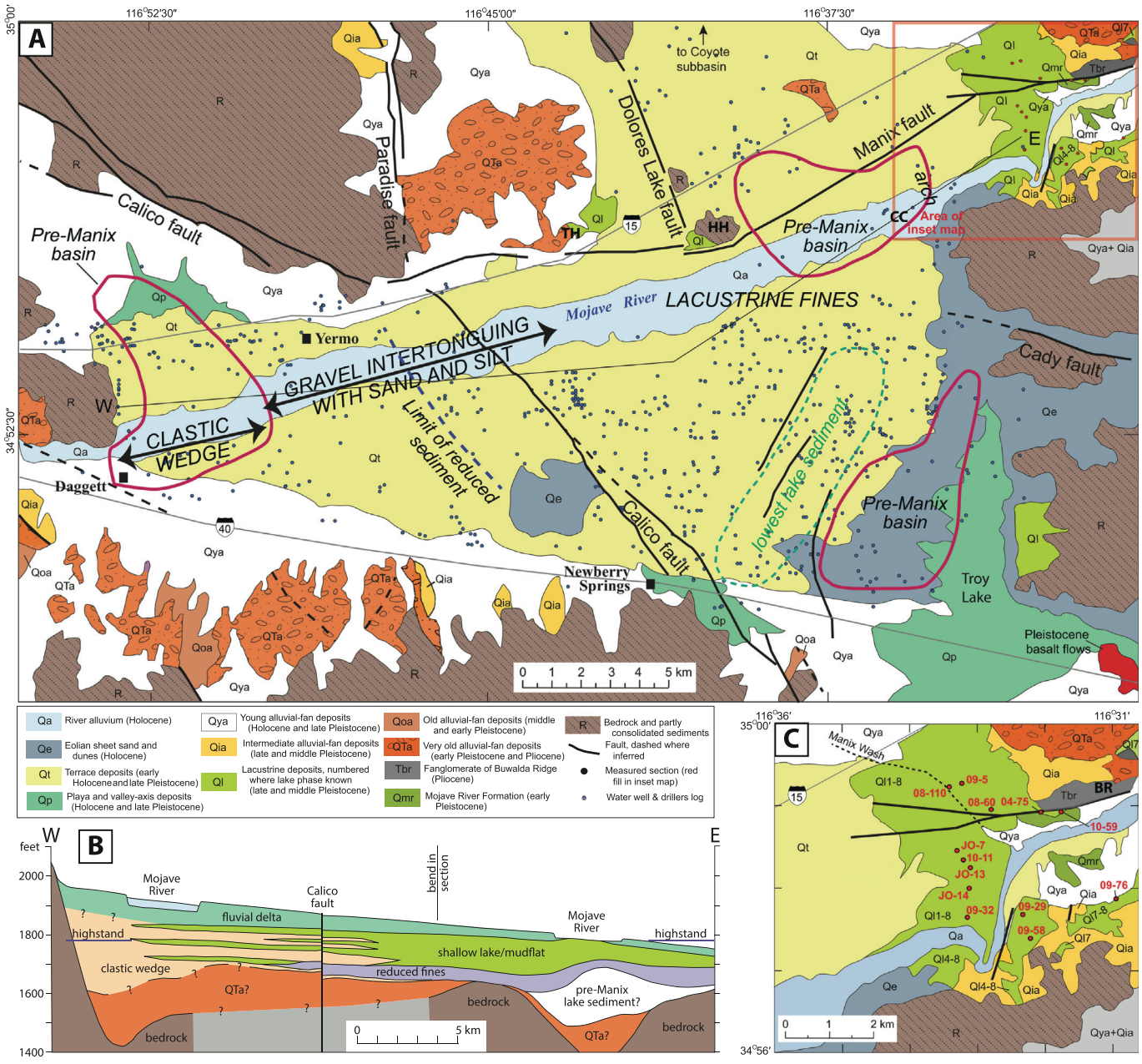

Fig. 4. Sketch maps and section of (A) Cady subbasin geology with emphasis on relations in the vicinity of the Manix Wash-Mojave River area, including locations of measured sections (denoted on inset map) and well logs. Red polygons enclose small basins that were probably present prior to the arrival of the Mojave River and formation of Lake Manix. Bold arrows summarize types of sediment present in the subsurface from well data. CC, Camp Cady; HH, Harvard Hill; TH, Toomey hill. (B) Stratigraphic profile depicts sedimentary units summarized from examination of well logs in the Cady subbasin and projected to a line from north of Daggett (W) to near Manix Wash (E). (C) Inset map expands the geology around the west end of Buwalda Ridge (BR) and the sill between the Cady and Afton subbasins. Site numbers (red dots) in this inset map are measured sections shown in Table 1 and Fig. 5.

makes a convenient marker for the Barstow Formation in well logs, and it can be shown that the overlying Lake Manix sediments in that area thicken eastward. Where the basalt pinches out, and in a few wells that extend below the basalt, more 'blue clay' and other evidence for lacustrine sediment is logged. In many places, drillers note more resistant clays or silicified beds in this interval that probably represents the Barstow Formation. This evidence, as well as that described by Miller et al. (2019) closer to Coyote Lake, makes the base of Lake Manix difficult to determine north of the Manix fault. We limited our analysis of the lake deposits in this region to the area where the basalt is present in well logs.

Lacustrine deposits are greater than 150 m thick in an area west of Troy Lake and 85 m thick near Camp Cady, both anomalous in comparison with the typical ~45 m thickness elsewhere. At Camp Cady, lacustrine sediments occur in the base of the Mojave River channel and overlying delta sediment in the north bank of the river can be followed more or less continuously eastward to the classic Lake Manix outcrops. In this area, the section thins across an arch (Fig. 4). We consider it unlikely that the section greatly thickens near Camp Cady. We suspect that the great thickness of lacustrine sediment at Camp Cady and Troy Lake includes significant pre-Manix deposits. This older lake or lakes could be a lacustrine facies of the Mojave River formation (~0.6–2.2 Ma) or even older deposits. At Camp Cady, sediments underlying the pre-Manix lacustrine deposits are similar to alluvial fan deposits elsewhere, and therefore we assign them to unit QTa, precluding a Miocene age for the pre-Manix lacustrine deposits for this basin.

In much of the central Manix basin, the base of the lake is well defined as 'blue clay' on clastic wedge gravel or bedrock. Across this

area, the lake deposits are commonly about 45 m thick. They are capped by deltaic deposits about 10–20 m thick, which thicken westward and are difficult to differentiate from clastic wedge deposits west of the Calico fault. To the southeast, the delta deposits thin toward the west edge of Troy Lake.

4.1.3. Reduced lake deposits

We mapped a reduced sediment package within the Lake Manix section in many well logs by noting mention of "blue clay." In some logs, more specific colors such as gray, green, and rarely black were described that we included in the reduced section. White was also mentioned, but we did not include it because enhanced carbonate or diatom content can cause white sediment. Sediment in the reduced section includes clay, silt, and sand. We correlate this reduced sediment interval with the lower part of the core studied by Reheis et al. (2012) and assigned to lakes 1 to 4 (Fig. 3; MIS 12 to 8), although specific correlations are not possible because of the different quality in the different data sets. Sparse detailed well logs show additional reduced beds above the main 'blue clay' zone, which agrees with the Manix core record. Sediment in the upper part of the lake record is more commonly oxidized, interpreted in the Manix core as mudflat and lenses of alluvial sediment, along with oxidized soils.

The top of the reduced sediment interval is defined east of the Calico fault by over 100 well records. Although not all drill records reliably identified the sediment, elevations in nearby wells show good agreement. The pattern is one of a fairly smooth decline in elevation southeastward across the basin from ~535 m to ~500 m. An interesting low that defines a narrow northeast-trending basin west of Troy Lake (Fig. 4) represents the lowest level for this horizon. It parallels mapped graben that were reactivated during the Landers earthquake in 1992 (Unruh et al., 1994). It is possible that the area has been subsiding as a small basin through the middle and late Quaternary. That the low existed during Lake Manix evolution is evident from unusual gravel deposits, repeated several times in well logs, that line the northeast-trending basin margins. These are the only gravel deposits noted in well logs east of the area shown as the clastic wedge and the intertonguing gravel and fines, most of which lie west of the Calico fault. The gravel fringing the narrow basin probably is sourced near Newberry Springs based on driller notes of volcanic rocks. At Newberry Springs, volcanic bedrock is at playa level and may have also been near lake level in early lake stages. We suggest that these gravel deposits represent beaches that were built along the edges of the narrow basin during transgressions and regressions. If so, they represent a persistent low in that area. The low is not evident in surface topography and was probably filled during delta and fluvial plain progradation toward the east, moving the depocenter eastward to present Troy Lake.

The westernmost pinchout of the reduced lake deposits is marked on Fig. 4, where it is represented by reduced sediment about 2 m thick, with a top at 489 m elevation. The lake may have been as deep as ~55–68 m at the time of deposition. Here, the reduced section lies above the initial clastic wedge gravel and within the first (lowest) tongue of fine sediment. Although the section in Fig. 4 shows the reduced lake sediments as being restricted to the earliest lacustrine tongue within the clastic wedge, at least one well log describes reduced sediments in the second lacustrine tongue.

In summary, the western area of Lake Manix is interpreted to be underlain by three preexisting basins. The small basin near Yermo was rapidly filled with Mojave River alluvium when the river arrived from upstream. These clastic sediments then prograded eastward as lacustrine sediments were deposited in the Troy Lake and Cady subbasins, which initially may have been separated by a low divide. The Troy basin was located about 5 km west of the margin of Troy Lake playa. Finally, Mojave River fluvial deposits blanketed most of this western area, including deltaic deposits of Lake Manix that extend to the west at least as far as Yermo. Beach ridges of Lake Manix are preserved on the western margin of the Cady Mountains, but exposures are limited and only one conventional radiocarbon age of 15,025 ± 230 ^{14}C yr B.P. has been obtained on *Anodonta* shells (Meek, 1990).

4.2. Outcrop stratigraphy of Cady Subbasin

The Manix Formation is well exposed along the Mojave River and its main tributary, Manix Wash, west of Buwalda Ridge (Figs. 2 and 4). These outcrops have long been targeted for stratigraphic and chronologic studies because they comprise the thickest exposed sequences of lake deposits and contain a wealth of vertebrate fossils (Buwalda, 1914; Jefferson, 2003). Jefferson (2003 and references therein) identified four mappable units that he viewed as lithologic facies (Fig. 3). From oldest to youngest, member A of the Manix Formation consists of partly lithified alluvial fan deposits composed of mafic volcaniclastics derived from the Cady Mountains to the south. Member A, herein referred to as the Cady fanglomerate, rests conformably on the uppermost arkosic sediments of the Mojave River formation (Nagy and Murray, 1991). This formation ranges from ~2.4 to 1.0 Ma based on tephra correlations and magnetostratigraphy (Pluhar et al., 1991; Miller et al., 2011; Reheis et al., 2014b). The fanglomerate interfingers near its top with the oldest lake sediments of member B, and locally, the uppermost gravel beds are coated with lacustrine tufa (Fig. 3; Nagy and Murray, 1991). Members B and C consist of interfingering fluvial and lacustrine deposits. Jefferson (2003) found that member B represented mostly nearshore and fluvial facies of the Manix Formation, whereas member C represented perennial-lake facies. He identified a basal and an intermediate wedge of member B interbedded with member C. The uppermost member D consisted mainly of arkosic sand and gravel deposited as fluvial and thin lake deposits under fluctuating lake levels as the Mojave River fluvial delta prograded eastward toward Manix Wash.

4.2.1. Lacustrine stratigraphy

Our stratigraphic sections and mapping, combined with the sedimentary sequence and age control from the Manix core as well as ostracode biostratigraphy, provide refinements to Jefferson's (2003) work. An important advance in subdividing the Manix Formation was our recognition of several buried soils in the deposits exposed in outcrop and in the core (Fig. 3). These buried soils are oxidized to 7.5 to 5 YR colors and locally have slickensided faces on vertical cracks; we interpret these features to represent subaerial weathering on desiccated lake sediment. The vertisols, combined with sedimentology and stratigraphy, define eight lake cycles (Ql1 through Ql8 in Fig. 3), three more than previously recognized (Jefferson, 2003). Some of the nearshore and fluvial deposits in outcrop (member B) are represented by muds deposited in a perennial lake in the core, apparently because of its more offshore location (for example, Ql3).

In the upper part of the sequence, particularly units Ql6 and Ql7, our interpretation differs from that of Jefferson (2003), who interpreted these sediments as muds of a perennial, relatively deep lake (his upper member C; Fig. 3). In addition to beds of massive to laminated lacustrine mud, this interval contains normally graded beds of sand, silt, and clay commonly having rip-up mud clasts at the base and mudcracks, locally with raindrop imprints, at the top (Reheis et al., 2012). These beds record flooding and desiccation events, including formation of weak soils, in a mudflat setting alternating with intervals of deeper water. Most of the exposures of unit Ql6 higher than 515 masl also display unique features close to the base of this unit (Fig. 5) including (1) a fining-up sequence of lacustrine sand and silt, truncated by (2) disturbed bedding, brecciated mud, and (or) mixed gravel, mud, and rip-up clasts of green mud (Fig. 6), overlain by (3) a buried soil, formed on either the disturbed deposits or a thin fan gravel (Figs. 5, 6A). Where the 184-ka Manix tephra is present, these features are always beneath the tephra and separated from it by a weak buried soil. The tephra itself occurs within lacustrine sediment below about 522 m and within mudflat sediment if present above that elevation. We interpret these disturbed features to represent an event involving

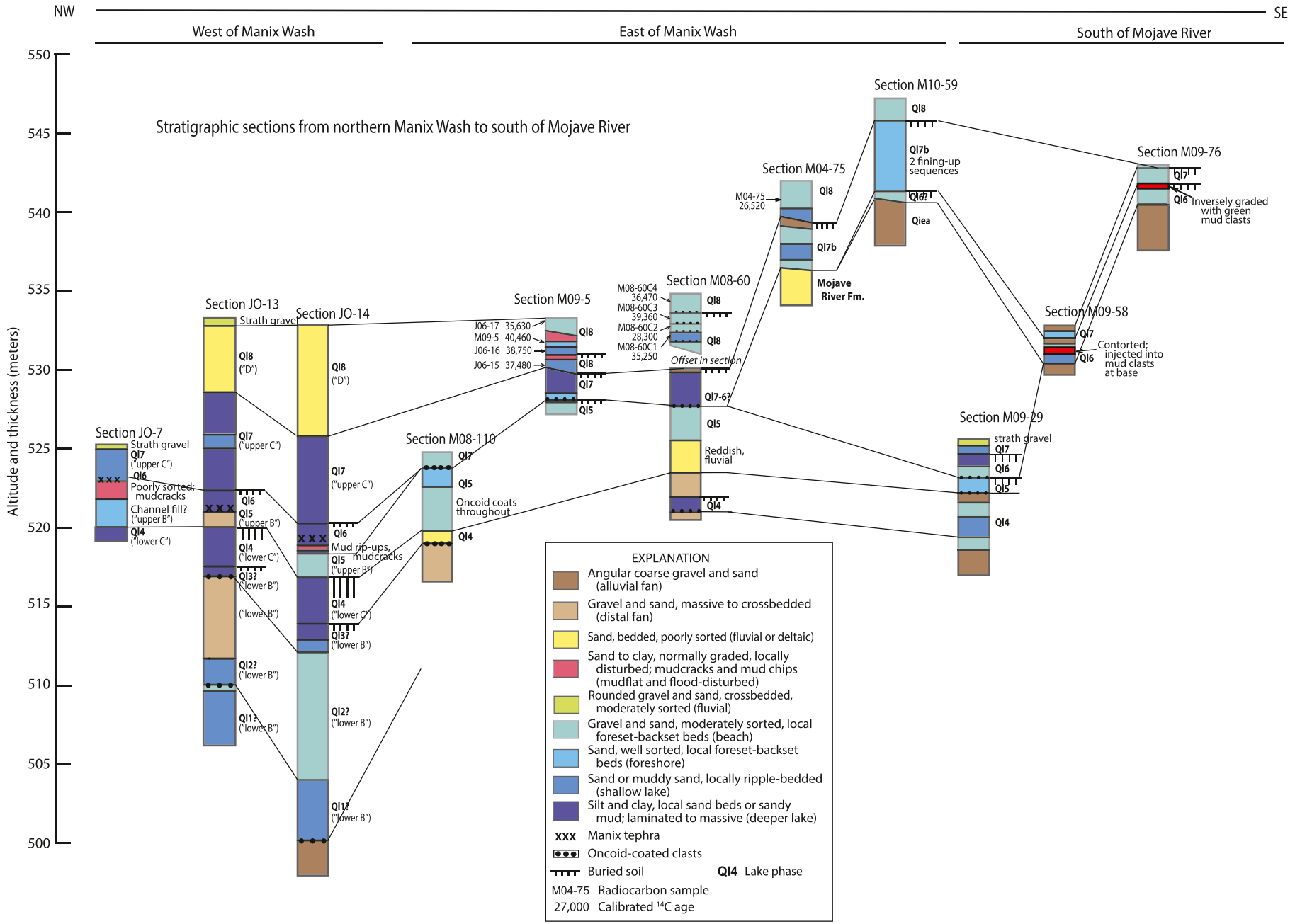

Fig. 5. Selected measured sections in the Cady subbasin, showing radiocarbon age control (see Reheis et al., 2014b, for sample information including errors on calibrated ages). See Table 1 and Fig. 4 for section locations. Most section tops and bases are true elevations measured by differential GPS.

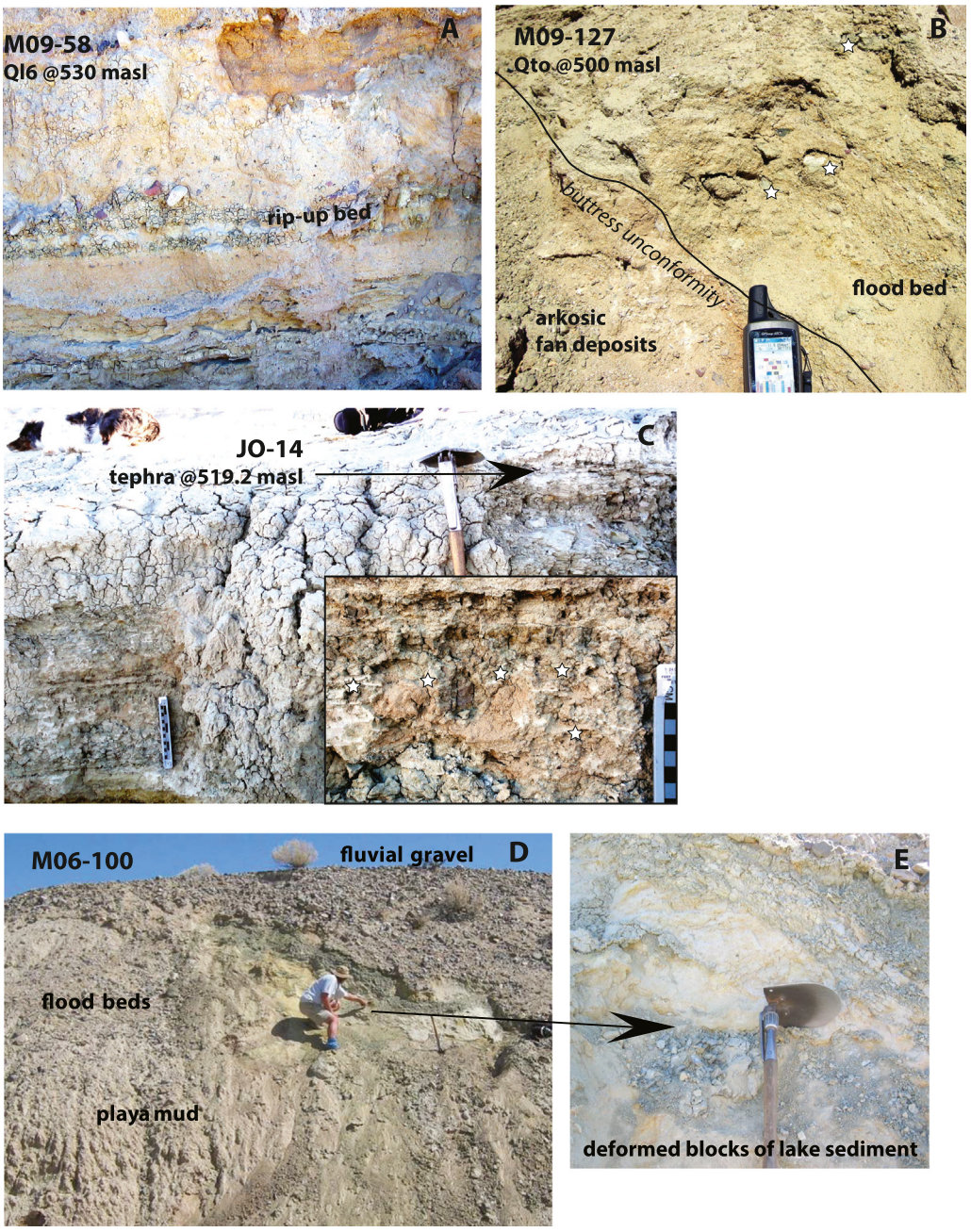

Fig. 6. Photographs of disturbed beds deposited in response to catastrophic integration of Afton subbasin. Stars indicate green lake-mud rip-ups in some photographs. See Table 1 for locations. A, rip-up bed of green mud clasts intermixed and interbedded with poorly sorted sand and gravel. Bed overlies well-bedded lacustrine deposits of unit Ql6 (at base) and is overlain by crossbedded sand with contorted bedding. South side of Mojave River, Cady subbasin. Section shown is ~80 cm thick. B, buttress unconformity cut on fan deposits on east end of Buwalda Ridge, east of former lake sill. Note green mud clasts in poorly sorted sand representing flood bed. GPS for scale. C, rip-up bed below Manix tephra on north side of Mojave River, Cady subbasin. Inset shows close-up of disturbed bed. Bed overlies transgressive lake sand, silt and clay of Ql6, and is capped by a thin brown cracked mud, in turn overlain by fining-upward silt and clay below tephra layer. Scale is 15 cm long. D and E, flood beds on north side of river in Afton subbasin. Beds overlie brown playa mud and are capped by fluvial gravel. Flood beds are dominated by large contorted clasts of semi-consolidated lake mud and sand as much as 3 m across, but also contain smaller blocks of playa mud. Shovel is 50 cm long.
All photos by M. Reheis.

pronounced desiccation that caused rapid lowering of lake level and remobilized sediment on slopes.

Biostratigraphy using ostracode species bolsters the correlation between outcrop and core in the older part of the section below the Manix tephra (Fig. 3). Within the core, ostracodes above 30 m depth (Ql4–Ql7) are exclusively *L. ceriotuberosa* (Reheis et al., 2012), which is a species tolerant of a wide range of temperature, salinity, and alkalinity, and is currently found in many U.S. and Canadian fresh-to-saline alkaline lakes (Forester, 1985; Forester et al., 2005b). Sediments of Ql3 and Ql2 are characterized by *L. platyforma* and *Limnocythere robusta*. Living specimens of *L. platyforma* have not been found (Delorme, 1971) so nothing is directly known about its ecological tolerances, but it is likely a low salinity variant of *L. ceriotuberosa* (Steinmetz, 1988; Reheis et al., 2012). To our knowledge, *L. robusta* is also extinct. Fossil valves of *L. robusta* have been found in association with *Limnocythere sappaensis* (saline, alkaline tolerant), *L. ceriotuberosa* (fresh-to-saline, alkaline tolerant) and L. *platyforma* (e.g., Cameron, 1971; Forester and Bradbury, 1981; Meek, 1999; Denison-Budak, 2010). Thus, the limited occurrence

of *L. robusta* in the Manix basin supports the fresh-to-saline, alkaline lacustrine paleoenvironmental interpretations inferred for the various Manix lake cycles (Reheis et al., 2012). Ql1 sediment is dominated by *Limnocythere bradburyi*, which tolerates a lower range of salinity and a comparable range of alkalinity as *L. ceriotuberosa*, but today lives only south of the Mexican border in shallow, predominantly freshwater alkaline lakes that receive summer rainfall maxima and where winter air temperatures rarely fall below freezing (Forester, 1985). We examined a 12.5-m section forming the base of the Manix Formation on the west side of Manix Wash (Fig. 4). The basal third of this section contained abundant *L. bradburyi*, and the upper third of the section contained mainly *L. platyforma* and *L. robusta*, identical to the sequence in the core. The section was capped by green lacustrine muds of "member C," which contains only *L. ceriotuberosa*. Similar species compositions and changes were found in part of lower "member B" (Steinmetz, 1987) at the reference section established by Jefferson (1985) on the Mojave River, but lacking the oldest unit containing *L. bradburyi*. We conclude that lower "member B" in outcrop is equivalent in age to the basal 13 m of the core (ca. 450–330 ka; Reheis et al., 2012) and represents lake units Ql1–Ql3 (Fig. 3).

AAR D/L values measured on ostracodes also provide broad correlation between the core and outcrop (Fig. 3; Table 2). D/L values for glutamic and aspartic acids for the eight core samples show a general increase with age from about 11.5 m depth to about 40.2 m depth, with the most distinct increase in values between 22 and 26 m. This break roughly corresponds with a similar sharp increase in the series of seven D/L values from outcrop samples that coincides with the position of a paleosol. The single sample analyzed from unit D in outcrop has distinctly lower D/L values, supporting a younger age for this unit and the correlative Ql8 phase.

The youngest unit Ql8 ("member D" of Jefferson, 2003) grades eastward from fluvio-deltaic deposits into nearshore lacustrine deposits exposed on the east side of Manix Wash (Figs. 4 and 5). These lake deposits lie above a vertisol formed on green mud of unit Ql7 and tend to coarsen upward from fine sand and silt to gravelly arkosic sand through several subunits. These subunits represent fluctuations in lake level and discharge and may be separated by transgressive oncoid-coated pebble layers and locally by lagoonal deposits of brown mud or very weak soils (Reheis et al., 2012, 2015).

4.2.2. Age control

The chronology of Lake Manix deposits in the Cady subbasin is derived from radiocarbon dates on *Anodonta* shells, tephrochronology, uranium-series dating on bone, oncoid tufa, and ostracodes, and an age model for the Manix core based on the above constraints combined with paleomagnetic data.

Calibrated radiocarbon ages (2σ) range from 29,470 (29,170–29,780) to 43,530 (42,600–44,580) cal yr B.P. in stratigraphic order in the fluvio-deltaic sediments in the upper ~7 m of section (Ql8) exposed along the Mojave River and Manix Wash. Overlapping ages from the equivalent beach and shallow lacustrine deposits along the east side of Manix Wash and a few places on the south side of the Mojave River range from 25,530 (25,280–25,740) to 41,670 (40,890–42,330) cal yr B.P. (Fig. 5; age ranges from Reheis et al., 2015).

The 184-ka Manix tephra lies in unit Ql6 in the core (Fig. 3), and can be traced nearly continuously along outcrop on the north side of the Mojave River and the west side of Manix Wash, but is rarely found at elevations higher than about 522 masl. The tephra was also identified at one location (34.950°, −116.558°) south of the river.

We obtained uranium-series age estimates on oncoid clast rinds from the base of the Manix core (sample MX30: 3–9 cm; Table 1; Fig. 3) and from Ql1 gravel and sand overlying the top of the Cady fanglomerate exposed along the Mojave River (sample JP-071006-1), as well as from ostracodes sampled from lower "member B" (sample Mnx_lowerB, Fig. 3) within the interval containing abundant *L. robusta* correlated to Ql2 in the core. Three of the six subsamples of oncoid carbonate from MX30 core had low U/Th values that required very large corrections for initial ^{230}Th, making them unreliable for age information (Appendix A, Table S1). The three subsamples with smaller corrections (U1, U2, and U4 in Table S1) yield detritus-corrected ^{230}Th/U age estimates of 146 ± 19 to 183 ± 33 ka, but with lower-than-expected initial [^{234}U/^{238}U] values of 1.15 to 1.21. Assuming this carbonate precipitated from paleo-lake water, it likely gained U at some time after burial resulting in lower [^{230}Th/^{238}U] values that yield erroneously young ^{230}Th/U age estimates considering the stratigraphic position of these

Table 2
Aspartic acid (Asp) and glutamic acid (Glu) D/L values in *L. ceriotuberosa*.

Lab ID (UAL)	Sample	Lake	n[a]	ex[b]	Asp D/L	1s	Glu D/L	1s
Core								
5818	MX-9-11.1	Ql7	7	5	0.47	0.02	0.30	0.02
5819	MX-14-19.4	Ql6	11	4	0.51	0.01	0.22	0.02
5820	MX-16-21.9	Ql5	12	2	0.48	0.01	0.24	0.01
5821	MX-18-25.9	Ql4	14	2	0.56	0.02	0.39	0.02
5822	MX-20-27.9	Ql4	13	1	0.56	0.02	0.36	0.02
5823	MX-22-31.2	Ql3	11	2	0.56	0.03	0.35	0.03
5824	MX-24-34.6	Ql2	8	2	0.62	0.02	0.46	0.04
5825	MX-28-40.0	Ql1	8	4	0.55	0.03	0.49	0.01
Outcrop								
4172	M03NS 1765	Ql8	6	1	0.42	0.02	0.19	0.02
4110	M03NS 1763	Ql7	12	2	0.45	0.03	0.30	0.03
4109	M03NS 1762	Ql6	10	2	0.48	0.02	0.25	0.01
4107	M03NS 1760	Ql4	9	3	0.54	0.00	0.39	0.01
4108	M03NS 1759	Ql4	13	1	0.51	0.02	0.37	0.02
4150[c]	Lower B	Ql3	9	1	0.57	0.02	0.39	0.02
Afton								
4149	Manix 471	Ql7	6	1	0.47	0.02	0.36	0.04
4382	JR04D-98B	Ql7	8	0	0.50	0.01	0.33	0.02
4972	JR05D-162B	Ql7	9	1	0.49	0.02	0.35	0.02
4973	JR05D-162C	Ql7	8	1	0.50	0.01	0.34	0.01
4377	JR04D-98CC	Ql7	8	0	0.50	0.01	0.29	0.02
4383	JR04CM-93 D-1	*	7	1	0.51	0.04	0.31	0.04
4389	JR04D-99A	Ql7	7	1	0.51	0.03	0.31	0.02

[a] Number of subsamples used to calculate the mean and standard deviation.
[b] Number of subsamples excluded.
[c] *L. platyforma*.
* Post-Lake Manix slackwater deposits; likely reworked from older sediment.

Table 3
Summary of U-series dates for samples used to constrain the Pleistocene history of Lake Manix (data from Table S1 in Appendix A).

Sample ID	Map unit	Sample type	Latitude, Longitude (degrees, WGS84)	U-series age ± 2 s (ka)	Age comment
M05-19J	Within Ql8	Tufa — rind on clast	35.0627 −116.4333	43 ± 4	Weighted mean ^{230}Th/U age; $N = 3$
M05-26C	Base Ql8	Thin rind on granite clast; small oncoidal nodules	35.0435 −116.3695	51 ± 15	Weighted mean ^{230}Th/U age; $N = 2$
M06-62B	Base Ql8	Thick, laminated oncoidal tufa crust	35.0295 −116.3864	51 ± 6	Weighted mean ^{230}Th/U age; $N = 5$
M05-25H	Within Ql7	Ostracode valves	35.0447 −116.3656	170 ± 30	Single ^{230}Th/U age on multiple valves
M06-145	Within Ql7	Laminated oncoidal tufa rinds on rock clasts	35.0403 −116.3554	187 ± 120	Isochron ^{230}Th/U age; $N = 4$
JR06D-202	Base Ql7	Thick, laminated oncoidal tufa	35.0322 −116.39416	133 ± 8	Weighted mean ^{230}Th/U age; N = 3
M05-19B	Base Ql7	Thin oncoidal tufa crust on clast	35.0630 −116.4339	181 ± 32	Weighted mean ^{230}Th/U age; N = 2
M06-50	Base Ql7	Crudely laminated oncoidal tufa rinds on rock clasts	35.0312 −116.3582	166 ± 12	Weighted mean ^{230}Th/U age; N = 5
M06-91a	Base Ql7	Thin, porous oncoidal tufa rinds on rock clasts	34.9852 −116.4980	150 ± 59	Weighted mean model ^{234}U/^{238}U age; N = 4
JP-071005-2	Within Ql6	Individual calcite-replaced rhizoliths	35.0490 −116.4250	173 ± 9	Weighted mean ^{230}Th/U age; N = 4
JP-071006-1	Base Ql2	Basal layers from thick oncoidal rinds on rock clasts	34.9539 −116.54806	403 ± 31	Single ^{230}Th/U age on most reliable analysis
Mnx_lower B	Base Ql2	Ostracode valves	34.9646 −116.5494	429 ± 82	Single model ^{234}U/^{238}U age on multiple valves
MX30: 3–9 cm	Within Ql1	Tufa — irregular nodule	34.9625 −116.5562	396 ± 71	Weighted mean model ^{234}U/^{238}U age; N = 3

samples some 23–25 m below the 184-ka Manix tephra (Fig. 4). Assuming this sample had an initial [^{234}U/^{238}U] of 1.39 ± 0.06 (Appendix A, Fig. S4), model ^{234}U/^{238}U age estimates for U1, U2, and U4 show similar values with large uncertainties of 378 ± 124 ka, 408 ± 119 ka, and 401 ± 132 ka, respectively. A weighted mean value for these three results yields a model ^{234}U/^{238}U age estimate of 396 ± 71 ka (Table 3), which is interpreted to represent the best U-series age estimate for original carbonate precipitation.

Ages for seven subsamples of basal laminae from four separate oncoid rinds collected as JP-071006-1 (Table 3) range from 87 ± 6 ka to 403 ± 31 ka (Table S1). However, subsamples with younger ages have initial [^{234}U/^{238}U] that are substantially lower those expected for paleo lake water. The one subsample with a consistent initial [^{234}U/^{238}U] value and the least amount of detrital contamination (sample JP-071006-1F1) yields a ^{230}Th/U date of 403 ± 31 ka, which we interpret as the best-age estimate (Table 3) for sediments at the top of the fanglomerate at this site. The other subsamples are suspected of open-system U gains causing erroneously young ^{230}Th/U age estimates. This interpretation is supported by model ^{234}U/^{238}U ages for all seven subsamples ranging from 333 ± 69 ka to 706 ± 122 ka (Table S1) and a weighted mean value of 470 ± 120 ka.

A single U-series analysis of multiple ostracode valves from fine-grained sediments of unit Ql2 located 2–3 m stratigraphically above the JP-071006-1 oncoid coats yielded a similarly old ^{230}Th/U age of 489 ± 147 ka with a slightly elevated initial [^{234}U/^{238}U] of 1.46 ± 0.17. A model ^{234}U/^{238}U age for the same analysis using an initial [^{234}U/^{238}U] value of 1.39 ± 0.06 (Fig. S4) is 429 ± 82 ka, which is considered the best-age estimate for this sample (Table 3). U-series age estimates of ~400–500 ka for both the oncoid carbonate and ostracode dates reported here are consistent with an infinite (>350 ka) age obtained by J. Bischoff (U.S. Geological Survey; reported in Jefferson, 2003) on camel bone about 6 m higher in the section, and with the correlated depth of those samples to age-depth models for the Manix core (Fig. 3).

Two age models were developed for the Manix core using radiocarbon dates from outcrop, the age of the Manix tephra, and a sequence of paleomagnetic excursions and intensity maxima (Fig. 3; Reheis et al., 2012). Both age models suggest that the base of the core extends to approximately 480–500 ka (beginning of MIS 12, 478 ka). The models indicate that lacustrine and fluvial deposits of the Ql7 phase in the core, and unit "upper C" of Jefferson in outcrop, extend from early MIS 6 to as young as MIS 4. The basal age is consistent with the next oldest known pluvial lake record upstream from Lake Manix, the Lake Hinkley deposits (Fig. 1), which include the Lava Creek B ash and are thought to range from ~640 ka to somewhat younger than 620 ka (Miller et al., 2020).

4.2.3. Distribution of lake sediment

Outcrops and water-well logs show that the Manix Formation is thickest in the area west and north of Camp Cady, and thins across an arch near the northeast corner of the Cady Mountains (Fig. 4), deepens farther east, and thins again toward the northern front of the Cady Mountains and to the northeast against Buwalda Ridge (Fig. 3). The exposed sequence, including fluvial sediment at the top, is as much as 40 m thick along the north side of the Mojave River (Jefferson, 2003; Oviatt et al., 2007). The adjacent Manix core contains 42.5 m of lake and fluvial sediment; water-well logs farther north near Interstate 15 (Fig. 4) suggest thicknesses as much as 60–90 m, and north of Camp Cady they record "blue clay" to depths of over 100 m. As described in Section 4.1, these records may in part include lake basins that predated Lake Manix. South of the river, exposed sequences (Fig. 5) as much as 14 m thick lie near the hairpin curve (34.9503°, −116.550035°) and include units Ql4–Ql8 intercalated with fan gravel shed from the Cady Mountains. Numerous north-striking faults (too closely spaced to depict on Fig. 4) cut these deposits, which thin greatly to less than 5 m thick within 1 km east of the hairpin, suggesting fault control of the lake margin in that area. Slivers and patches of sediment mapped as units Ql6–Ql8 (Reheis et al., 2014b) are preserved along the faulted southern face of Buwalda Ridge for about 2 km east of Manix Wash. Along the southern margin of the large abandoned meander south of the river (34°58″N, 116°31″W), the same three units, here less than 3 m thick (section M09-76, Figs. 4 and 5), lap onto a thick wedge of Cady fanglomerate that extends northward in a sharp promontory, defined here as the boundary between the Cady and Afton subbasins.

Lake unit contacts mapped around the Cady subbasin (upstream of the Buwalda sill) define the ranges of depositional elevations of each unit. These data constrain maximum lake level and sedimentation (Table 4; Fig. 5). Very limited exposure of units Ql1–Ql3 prevents such analysis for these early lake phases, but including the intervening alluvial deposits, they aggregate 12 m in the core and in a nearby outcrop.

Table 4
Elevations and thicknesses of lake units in Cady and Afton subbasins.[1]

Lake unit	Elevation of base (m)	Elevation of top (m)	Max. thickness (m)
Cady subbasin			
Ql4 ("lower C")	507–521, 536*	520–532	6–7
Ql5 ("upper B")	510–525	512–529	4
Ql6 (pre-flood)	510–537	513–541	2
Ql6 (post-flood)	512–522	513–522	2
Ql7 ("upper C")	514–540	515–555	12
Ql7 beach gravel	n.d.	546–558, 564*	n.d.
Ql8 ("D")	522–545*	535–544, 547*	13
Afton subbasin			
Ql66	461–512	472–513	10
Ql7	470–547, 558*	501–550, 560*	17
Ql7 beach gravel	n.d.	545–559, 564*	n.d.
Ql8	494-544	515–544	19

[1] Data summarized from many outcrops and measured sections (most are in Figs. 5 and 8).
* Altitude likely altered by faulting or tilting.

Unit Ql4 crops out extensively both north and south of the river and along Manix Wash. Excluding one location on a fault, Ql4 ranges from 507 to 532 masl. Ql5, a lesser lacustrine phase, represents mainly nearshore deposits intercalated with alluvial sediment and reached a maximum of 529 masl. We subdivide Ql6 based on the disturbed bed observed in many outcrops. Ql6 exposures of beds that include these disturbed sediments extend as high as 541 masl, whereas Ql6 beds above the disturbed sediment, including the Manix tephra, lie at elevations less than 522 m. Ql7 beds range from 514 to 555 masl, and beach ridges correlated with this unit range from 546 to at least 558 masl. Unit Ql8 ranges from 522 to 545 masl.

4.3. Afton Subbasin

The Afton subbasin is bisected by the Mojave River (Fig. 2). The Manix Formation is present on both sides of the river but is thicker and more extensively preserved to the north. The lake deposits overlie and are intercalated with arkosic alluvial fan deposits on the north side of the river and with mafic fan deposits on the south side. Ellsworth (1932) and Meek (1989b, 1994) showed that a fanglomerate derived from Cave Mountain prograded south across the present river course and was later buried by a volcaniclastic fanglomerate that prograded northward from the Cady Mountains. A tephra found within the upper part of the Cave Mountain fanglomerate is tentatively correlated with the 2.4-Ma Ishi Tuff (Reheis et al., 2014b).

4.3.1. Stratigraphy

Three lake units compose the Manix Formation in Afton subbasin, rather than the two identified by previous workers (e.g., Ellsworth, 1932; Meek, 1994), and are correlated with units Ql6, Ql7, and Ql8 (Fig. 3; Reheis et al., 2014b). The oldest unit consists of fluvial and lacustrine sediments that are as much as 15 m thick along the valley axis north of the river near Dunn siding (site M06-77, Figs. 7 and 8) and thin rapidly northward and eastward to as little as 50 cm thick as they rise up along the preexisting fan slopes. The fluvial deposits along the basin axis, mapped as unit Qto (unit Qof of Reheis et al., 2014b), overlie distal-fan and playa deposits and locally include several meters of chaotically bedded boulders of semi-indurated green lake sediment and brown playa mud (Fig. 6D, E). To the southwest, as far as the eastern end of Buwalda Ridge, this 10-m fluvial sequence consists entirely of crossbedded gravel and sand with northeasterly dipping beds containing common rip-up clasts and sand-sized grains composed of green mud. In one long exposure (M08-45; Table 1), unit Qto is divided into two depositional units by a weak buried soil. To the northeast between Dunn wash and Afton Canyon, similar fluvial deposits are interbedded with, and overlain by, lacustrine sand, silt, and thin green mud layers; these muds contain ostracodes of the same species present in the Cady subbasin. In some beds, green sand-sized clay aggregates are abundant. At one critical locality north of the river (site M07-159, Table 1, Figs. 7 and 8), fine-grained deposits 2.5 m above the base contain thin lenses of reworked Manix tephra, thus firmly tying these deposits to unit Ql6 in the Manix subbasin. South of the river, unit Ql6 is at least 4 m thick. Unit Ql6 is separated from Ql7 by fan gravel (Qia6, Fig. 7), commonly less than 1 m thick and locally bearing a very weak soil.

Unit Ql7 is as much as 17 m thick north of the river (DI, Dunn Island section, Table 1, Figs. 7 and 8) and about 12 m thick at one site south of the river (Tables 2–4 in Meek, 1990). Stratigraphic studies (Reheis and Redwine, 2008; Reheis et al., 2014b) show that shorelines higher than the late Pleistocene highstand (~543–544 m) likely correspond with deposits of unit Ql7. In axial-basin positions, Ql7 consists largely of laminated to massive green mud containing abundant ostracodes, intercalated with thinner (a few centimeters to 1 m) well-bedded sands (Reheis et al., 2012). On the east side of the North Afton beach ridge, unit Ql7 changes character: some outcrops display thick beds of beach gravel along the basin margin, and many exhibit lake-modified alluvial deposits of an active fan-lake margin (Reheis and Miller, 2010). In this area, the Ql7 lake rose on an alluvial fan complex on the steep western flank of Cave Mountain, and the style of deposition shifted repeatedly from that of coarse-grained, angular clast-supported and debris-flow beds with depositional slopes of 5–7°, and buried soils formed during periods of stability, to shoreline-modified fluvial beds (Reheis et al., 2007; Reheis and Miller, 2010). Some sites expose the architecture of a Gilbert-type fan-delta and sub-lacustrine bar, whereas others show alluvial fan deposits interfingering with nearshore sand and gravel. Southeast of Dunn wash and west of the North Afton beach ridge, many outcrops display a hiatus within unit Ql7 marked by a thin fan gravel bearing a weak buried soil. The hiatus is observed above ~495 masl; lower, this zone is marked by beds of nearshore lacustrine sand (e.g., DI section, Fig. 8). The boundary of units Ql7 and Ql8 is nearly everywhere marked by fan gravel 1–2 m thick with a prominent buried soil formed in it (Qia7). Dissection in response to incision by the Mojave River has commonly stripped Ql8 sediment down to this fan gravel, which forms extensive exhumed surfaces around the Afton subbasin (Meek, 1990, 2000; Reheis and Redwine, 2008).

Unit Ql8 is dominantly composed of beach sand and gravel where preserved in the Afton subbasin (Figs. 7 and 8). Beach deposits as much as 20 m thick underlie the North Afton beach ridge, and they rest on a subjacent fan surface, capping Ql7 deposits, which can be traced eastward to the basin margin. A prominent beach ridge is also preserved on the northeastern lake margin adjacent to Interstate 15, and other beach remnants are scattered around the Afton subbasin. Some Ql8 deposits were formed in active alluvial fan settings; in such locations, they are characterized by sediments that strongly resemble clast-supported alluvial fan sediments. However, close examination reveals that in some beds, the sediments have been modified by lacustrine processes, have oncoid tufa coats on clasts, and (or) contain fossils such as *Anodonta* shells and ostracodes (Reheis and Miller, 2010). Such sequences are well exposed in the upper reaches of Dunn wash (Reheis and Redwine, 2008). We have identified finer-grained silty and muddy beds 2–3 m thick, representing offshore deposition, in only two locations north of the river (Reheis et al., 2014b); elsewhere, these nonresistant beds have been eroded. As in the Cady subbasin, numerous subunits marked by transgressive oncoid-coated pebble layers, lagoonal muds, and very weak soils indicate lake-level fluctuations.

4.3.2. Age control

Ages of Lake Manix deposits in the Afton subbasin are based on radiocarbon and uranium-series dating, as well as the presence of the Manix tephra at one site in Ql6 deposits north of the river (Figs. 7 and 8). Calibrated radiocarbon ages on *Anodonta* shells from Ql8 deposits range from 24,460 (24,210–24,810) to 43,020 (41,960–44,320) cal yr B.P. (Reheis et al., 2015). We dated shells from a few Ql7 deposits and obtained ages near the upper limit of the method ranging from 40,000 to almost 50,000 ^{14}C yr B.P. (not calibrated) Given their stratigraphic positions below buried soils marking the unconformity at the base of Ql8 deposits, we interpret these as minimum-limiting ages for Ql7 (Reheis and Redwine, 2008; Reheis et al., 2014b).

Uranium-series best-age estimates were obtained on oncoidal rinds and crusts coating transgressive lake gravels of units Ql7 and Ql8, on one sample of rhizoliths from unit Ql6, and on one sample of multiple ostracode valves from Ql7 (Table 3). For unit Ql8, best-age estimates ranged from 51 ± 6 ka based on five subsamples of oncoidal tufa coating clasts from the base of the unit south of the river (sample M06-62B; Table 1, Fig. 7) to 43 ± 4 ka for three subsamples from a clast rind (sample M05-19J), the latter representing a younger lake rise within Ql8 north of the river (Figs. 7 and 8). We note that Meek (2000, 2015) reported a U-series age of 80 ka from samples at this same site but provided no analytical data. We have found no evidence to support an MIS 4 age for basal sediments of Ql8. Subsamples from two small, rounded oncoid nodules (sample M05-26C) from within Ql8 sediments have a mean ^{230}Th/U age estimate of 51 ± 15 ka (Table 3); however, their rounded

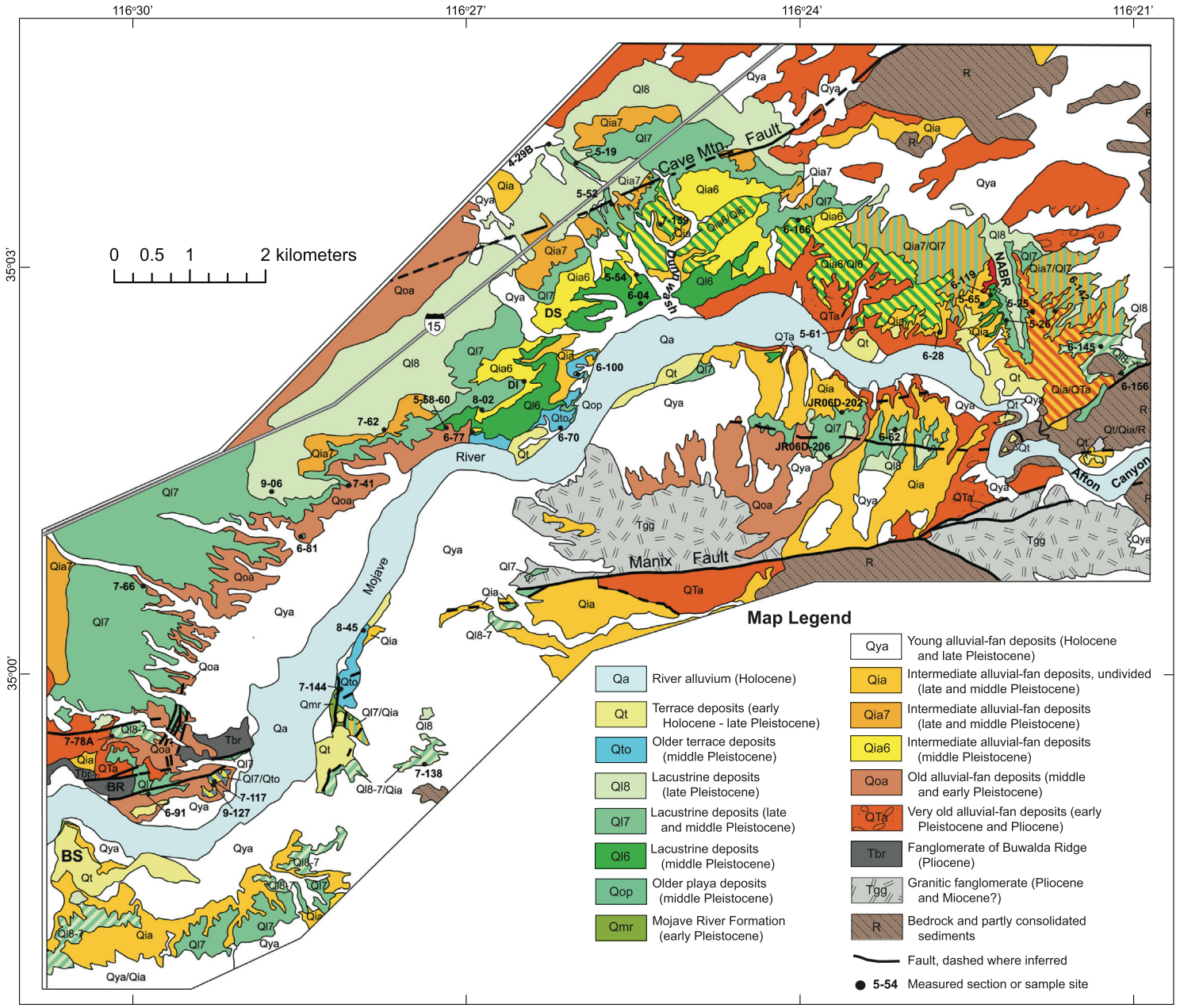

Fig. 7. Surficial geologic map of Afton subbasin, showing locations of measured sections and other sites (Table 1). BR, Buwalda Ridge; DS, Dunn siding; NABR, North Afton beach ridge. Large BS in lower left marks beveled surface representing location of former Cady-Afton sill. Striped areas are polygons of mixed units of the two colors, further denoted as, for example, Ql7/Qto if a thin veneer of younger unit overlies older unit, and as Ql8-7 if area contains younger and older units too small to be separately mapped at this scale.
Modified from Reheis et al. (2014b).

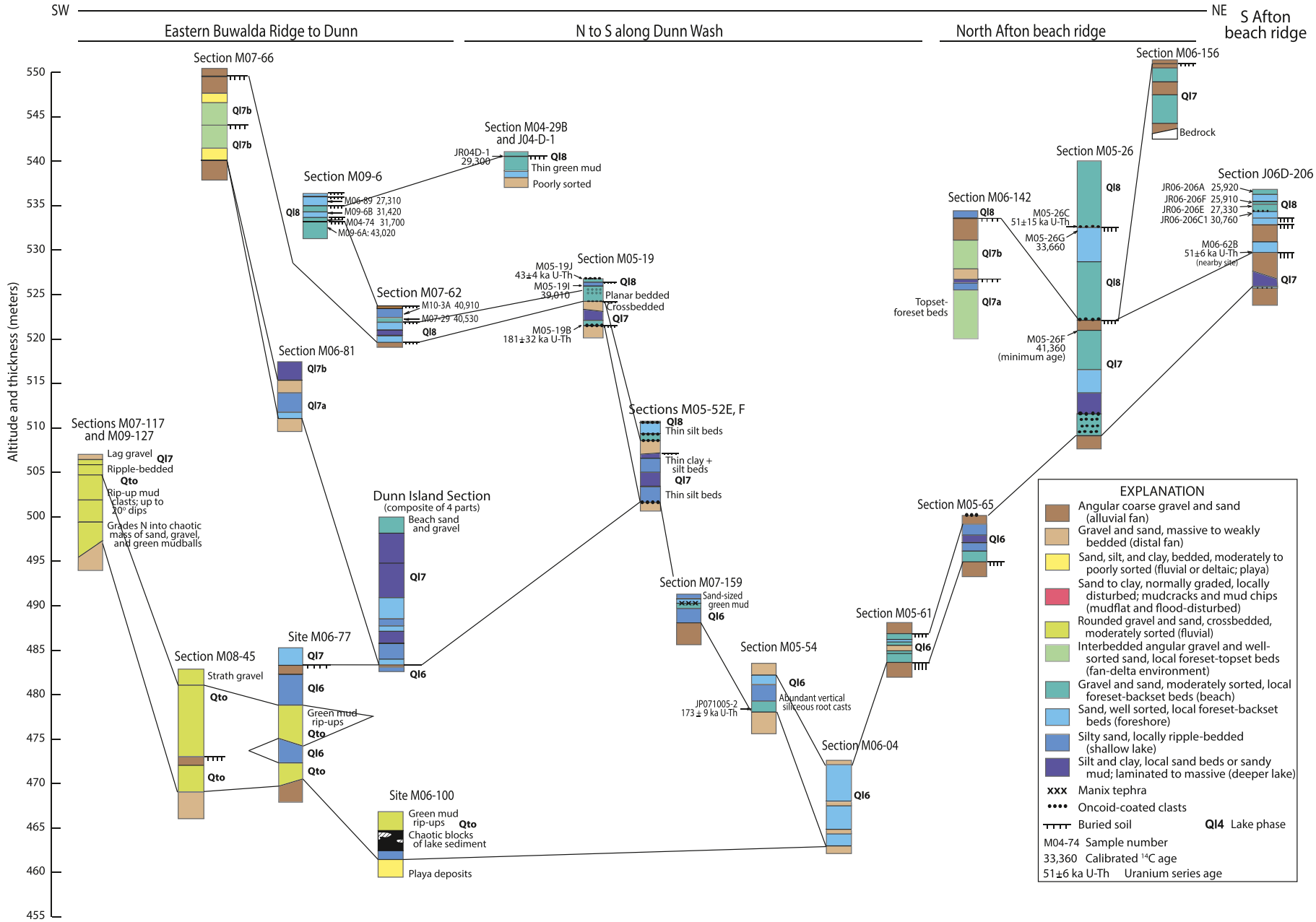

Fig. 8. Selected measured sections in the Afton subbasin, showing radiocarbon and U—Th age control (see Reheis et al., 2014b, for ^{14}C sample data including errors on calibrated ages and Table 2 for U—Th sample data). See Table 1 and Fig. 7 for section locations. Most section tops and bases are true elevations measured by differential GPS.

morphology likely indicates reworking of older tufa as clasts in Ql8 sediment overlying shells radiocarbon dated at 33,660 (33,230–34,010) cal yr B.P. (Fig. 8).

Significantly older ages were obtained from a series of oncoidal tufas and ostracode valves collected within and at the base of unit Ql7, and rhizoliths from within Ql6 sands (Appendix A). Best-age estimates are generally imprecise, ranging from 133 ± 8 ka to 187 ± 120 ka (Table 3). Basal carbonate layers from three specimens of oncoidal tufa (sample JR06-202; Table 1, Figs. 7 and 8) having thick, least-porous textures yield individual ^{230}Th/U age estimates of 144 ± 44 ka, 137 ± 18 ka, and 132 ± 9 ka (Table S1). Subsamples of microstratigraphically younger layers can have dates as young as 107 ± 5 ka while maintaining initial [^{234}U/^{238}U] values expected for paleo-lake water, introducing the possibility that tufa layers continued to accrete by displacive growth of calcite from porewater after clasts were buried in fine-grained sediments. Outer layers with ^{230}Th/U ages as young as 47 ± 14 ka have lower initial [^{234}U/^{238}U] (Appendix A) and are suspected of suffering U gains resulting in lower [^{230}Th/^{238}U] values and erroneously young ^{230}Th/U dates. The weighted mean ^{230}Th/U age of 133 ± 8 ka determined from three individual specimens is considered the best-age estimate for initial deposition of the thick, complex oncoid JR06-202 crusts sampled from Ql7 (Table 3).

Other oncoidal tufa rinds from Ql7 sediments have older ^{230}Th/U best-age estimates ranging from 166 ± 12 to 181 ± 32 ka (Table 3) with reasonable initial [^{234}U/^{238}U] values. Four subsamples from M06–145 within Ql7 sediments have substantially larger common Th contents despite their "detritus-free" appearance (Appendix A). Although reasonable estimates of the authigenic carbonate component could not be calculated, a poorly constrained three-dimensional isochron ([^{230}Th/^{238}U]-[^{234}U/^{238}U]-[^{230}Th/^{238}U]) yielded a consistent, but highly imprecise, ^{230}Th/U age estimate of 187 ± 120 ka with a reasonable initial [^{234}U/^{238}U] value of 1.33 ± 0.17. Subsamples of thin oncoidal tufa rinds coating several clasts from section M06-91A at the base of Ql7 (Table 3) yielded anomalously old ^{230}Th/U ages (251–355 ka) compared to other Ql7 samples as well as much higher initial [^{234}U/^{238}U] values (1.53–1.72; Table S1). Those carbonate rinds are suspected of post-depositional U loss. Assuming these samples precipitated from paleo-lake water with an initial [^{234}U/^{238}U] value of 1.39 ± 0.06 (Fig. S4), model ^{234}U/^{238}U ages for the same three analyses with the least detrital contamination range from 145 ± 111 to 157 ± 105 ka, yielding a weighted mean value of 150 ± 59 ka (Table 3).

A single analysis on a very small sample (3.0 mg; M05-25H) of multiple ostracode valves collected from within unit Ql7 on the North Afton beach ridge (Table 1, Figs. 7 and 8) yielded a ^{230}Th/U age estimate of 170 ± 30 ka (Table 3), similar to other Ql7 U-series dates. The resulting initial [^{234}U/^{238}U] of 1.34 ± 0.05 is within the range of values expected for U dissolved in paleo-lake water, providing some confidence that the thin carbonate shells have not been greatly affected by post-depositional U mobility. The large uncertainty for this single analysis does not allow more precise correlation between this and other Ql7 horizons.

Ql7 deposits are stratigraphically younger than the 184-ka Manix tephra and represent a large perennial lake (Figs. 5 and 8; Reheis et al., 2012). U-series ages for carbonate samples in the Afton subbasin form a cluster of dates that are largely consistent with that stratigraphic constraint. Five of the six results in Table 3 (excluding the younger 133 ka age for JR06-202) yield a weighted average U-series age of 168 ± 10 ka (95% confidence limit with a probability of fit of 0.87). Although weighting favors dates with smaller errors, a straight, unweighted average is very similar (171 ± 29 ka at 2σ). Samples representing Ql7 units were collected at different locations and elevations and likely reflect a more complex history of water-level fluctuation than can be resolved

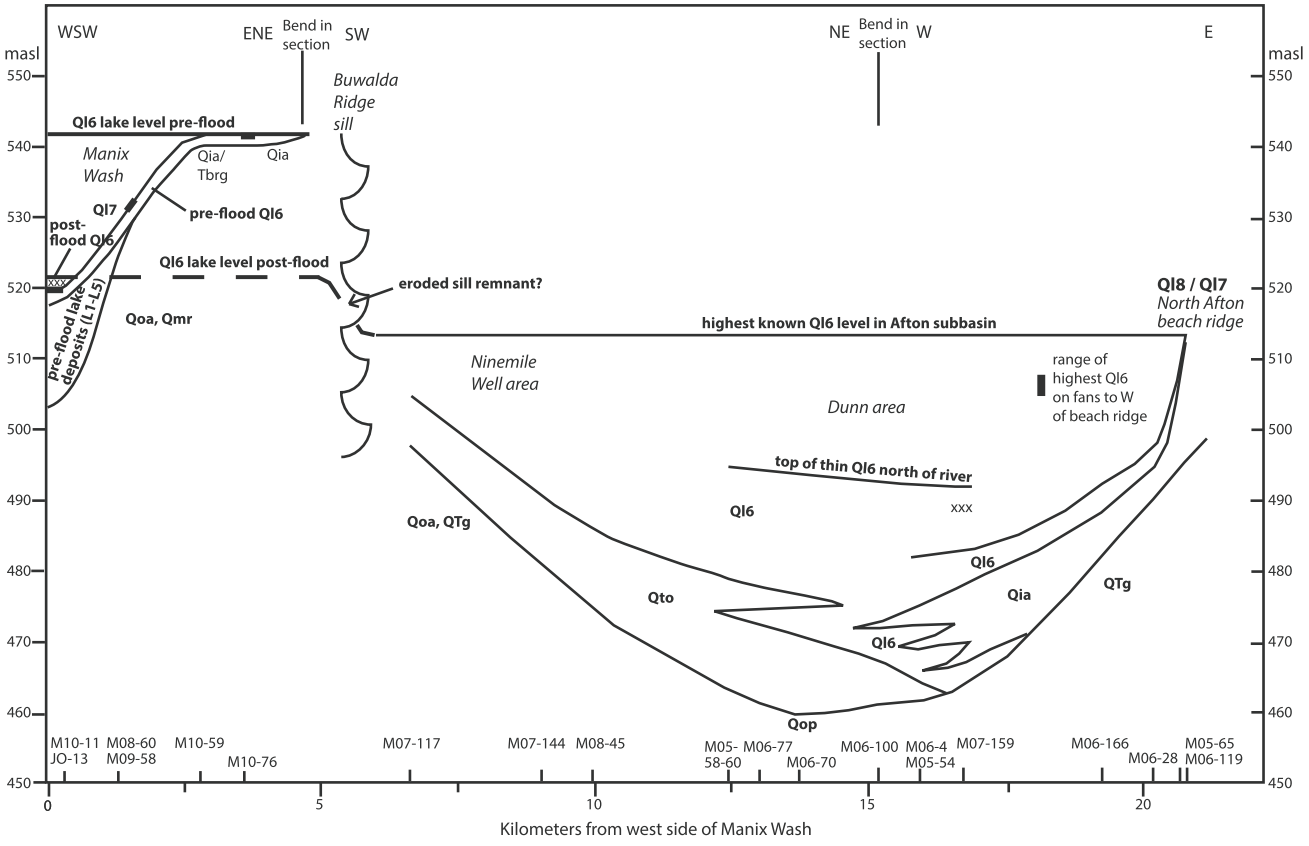

Fig. 9. Reconstructed thicknesses of Ql6 sediment and pre- and post-integration lake level in Afton and Cady subbasins. XXX marks two locations of Manix tephra. Thick black lines west of sill represent flood-disturbed sediment (see measured sections in Figs. 5 and 8 for details; locations in Table 1). Unit thicknesses derived from measured sections whose projected locations are shown along the line of section at bottom. Dashed line at 522 masl shows inferred Ql6 lake level west of the former sill after integration.

with these U-series ages. Nevertheless, results reported here are consistent with the presence of a substantial and widespread Ql7 lake phase early during MIS 6 time.

The only sample of carbonate material from unit Ql6 dated by U-series was a suite of small rhizoliths (sample JP-071005-2) collected from a bed of lacustrine sand about 1.2 m above the unit base (Tables 1 and 3, Fig. 8). Individual rhizoliths were replaced with authigenic carbonate having much higher U concentrations than oncoidal tufa (35–125 μg/g versus <10 μg/g; Table S1) and yielded a wide range of ^{230}Th/U age estimates ranging from 197 to 19 ka. However, initial [^{234}U/^{238}U] values for those also varied widely (1.26–1.53), causing suspicion of secondary losses and gains of U. Four of the eight analyses with initial [^{234}U/^{238}U] values between 1.43 and 1.46 had ^{230}Th/U ages ranging from 168.5 ± 1.8 ka to 181.8 ± 2.2 ka, which yielded a weighted mean ^{230}Th/U best-age estimate of 173 ± 9 ka (Table 3). That date is not statistically different than estimates obtained from Ql7 samples noted in the previous paragraphs. Although the rhizoliths originated as plants rooted into the basal unit of Ql6 that is presently below a carbonate-cemented zone and overlain by 3 m of lacustrine sand with no rhizoliths, final replacement of organic root matter and filling of any associated void space may have only occurred after lake levels returned to this elevation later during Ql7 time. Therefore, the best-estimate U-series date of 173 ka for the rhizoliths is considered to be a minimum for the timing of Ql6 deposition. This minimum age estimate is consistent with the 184 ± 4 ka Manix tephra within Ql6 deposits 1.5 km to the north.

We measured AAR D/L values on ostracode samples from the Ql8 and Ql7 phases (Table 2) to help correlate units between the Afton and Cady subbasins. Both sets of Afton samples yielded AAR D/L values that were higher than their correlative deposits in the Cady subbasin. These results suggest a systematic offset that may be the result of surface heating of the outcrops after they were exposed by erosion in this hot desert climate.

4.3.3. Distribution of lake sediment

In the Afton subbasin, the Manix Formation in outcrop is thickest along both sides of the river near Dunn siding (Figs. 7–8). These relations, and the presence of playa deposits beneath Ql6 deposits in this area, indicate that the modern valley coincides with the former basin axis. Measured sections show that the initial deposition of unit Ql6 and the intertonguing fluvial deposits of unit Qto to the west, both as much as 10 m thick (Table 4, Fig. 9), occurred within this basin axis. The base of the fluvial deposits rises gradually westward over 8 km from 460 masl near Dunn siding to 496 masl on the southeast margin of Buwalda Ridge. Intercalated thin fan gravels in several of the Ql6 sections suggest brief fluctuations in a generally rising lake. The highest remnants of Ql6 are found on the western flank of the North Afton beach ridge (Figs. 7 and 8) and on dissected slopes near Dunn wash extending up to 513 masl.

Erosional remnants of unit Ql7 are also thickest near and south of Dunn siding and thin in all directions from the basin axis. Elevations of deposits of this age range from 470 to as much as 550 masl. Few beach barriers of this unit with recognizable morphology are preserved in the Afton subbasin, with the exception of one likely beach ridge (M07-78, 554 masl) and a few surfaces of anomalously well rounded gravel near the northeastern flank of Buwalda Ridge and east of the ridge across the river (M07-138, 553 masl; Fig. 7, Tables 1 and 4; Reheis et al., 2014b). However, one site on the eastern edge of the basin (M06-156, Figs. 7 and 8) exposes nearly 6 m of lacustrine sand and interbedded fan gravel extending as high as 550 masl (Table 4; Reheis and Redwine, 2008). In many basin-margin locations, green mud of unit Ql7 can be traced upslope to lie beneath the 543-masl beach barriers of the younger Ql8, suggesting that the corresponding beach gravel of unit Ql7 must have been higher than 543 m and was largely eroded during deposition of the overlying fan deposits preceding the Ql8 lake rise.

Deposits of unit Ql8 range from 494 to 544 masl in the Afton subbasin (Table 4). Where not protected by gravel, most Ql8 deposits have been removed by erosion. They are as much as 18 m thick beneath the North Afton beach ridge (Fig. 8). This beach ridge is rooted on underlying Ql7 and older fan deposits and extends nearly 2 km with a gentle southward surface slope (Fig. 7), suggesting it was constructed as a spit by longshore currents transporting gravel derived from alluvial fans draining the west side of Cave Mountain. The configuration of this major feature, which points directly at the position of the former lake sill, may indicate occasional spilling of Lake Manix eastward during Ql8 time (Reheis and Redwine, 2008).

4.4. Coyote subbasin

The Coyote subbasin lies northwest of the Cady subbasin (Fig. 2), from which it is separated by a broad, nearly flat divide at ~540 m elevation floored by Mojave River distributary deposits (Meek, 1994; Dudash, 2006; Miller et al., 2018). In a few places, Miocene and Pliocene deposits rise above this surface and trenches indicate that similar deposits may be present in the shallow subsurface. This divide has played an important role in the rise of Lake Manix each pluvial cycle because the lake has a much larger evaporative surface after Coyote subbasin is joined, limiting the rate of rise above the level of the divide (Meek, 1994). Ancient lacustrine deposits in and near the playa floor are MIS 3 and older (Reheis et al., 2015) but their distribution and ages are difficult to interpret because the apparently limited time intervals of lake filling merely, but importantly, indicate the times of Lake Manix reaching near its highstand. A study of the post-Lake Manix late Pleistocene fluvial and lake history of Coyote basin by Miller et al. (2019) demonstrated that the ancestral Mojave River flowed directly to the Coyote basin at least once during MIS 3, on the basis of a thick wedge of sand derived from the San Bernardino Mountains and dated at well before the demise of Lake Manix at ~25 ka. Latest Pleistocene diversions of the river to Lake Coyote were influenced by earthquake scarps along the Dolores Lake fault (Fig. 4), and this mechanism may have influenced the MIS 3 river as well.

5. Evolution of Lake Manix

The Manix basin has undergone extensive geologic and geomorphic modification since the late Pliocene-early Pleistocene (Miller et al., 2011). Early in its history, it was separated into three major subbasins. The Cady and Afton subbasins of Lake Manix were separated by the massive Pliocene fanglomerate that forms Buwalda Ridge astride the Manix fault (Fig. 2). Alluvial fan and playa deposits record separate histories, which include the early Pleistocene Mojave River formation in the two subbasins (Nagy and Murray, 1991, 1996) and similar, less well studied deposits in the Afton subbasin, which may extend from the late Pliocene to the early middle Pleistocene (Figs. 4 and 7; Reheis et al., 2014b). The Coyote Lake subbasin formed during the early Pleistocene as older basin-fill deposits of Miocene and Pliocene age were folded into a broad sag in tandem with the uplift of the Alvord Mountains (Miller et al., 2011). This older tectonic history underpins the processes and events that shaped the evolution of the Lake Manix basin after the arrival of the Mojave River in the early-middle Pleistocene. The main processes include (1) infilling of the lake basin, (2) interaction among the subbasins as controlled by internal sills, and particularly the integration of Afton subbasin, (3) tectonics, and (4) climate change. Below, we discuss these interacting processes that resulted in the modern configuration.

5.1. Effects of sediment infilling

A fundamental control on evolution of the Manix basin has been the sediment load delivered by the Mojave River and deposited in a clastic wedge, its prograding fluvial delta, and more distal fines on the lake

bottom. Sediment progradation and aggradation initiated the downstream integration process by reducing the basin's water-holding capacity, eventually causing overflow into neighboring basins (Meek and Douglass, 2001). The Mojave River drains a large area of weakly consolidated granitic sediment in its headwaters in the Transverse Ranges and traverses the Victorville basin (Fig. 1), which served as the first terminus of the river during Pliocene and early Pleistocene time until after deposition of the 760-ka Bishop ash (Cox et al., 2003). After it escaped the Victorville basin, the river began reworking and transporting this basin fill. The river flowed initially to the Harper Lake basin (Cox et al., 2003; Miller et al., 2020), but later diverted to a more easterly course to Hinkley basin. Later, it incised the Lake Hinkley deposits as it carved a canyon near Barstow, where it entered the western end of the Lake Manix basin near Daggett (Fig. 4). Initial river deposits included voluminous gravel eroded from upstream clastic wedges of previous lake cycles as well as from adjacent alluvial fans. No age control is available for the timing of this event, but it must have occurred by ~480 ka, according to the Manix core chronology (Reheis et al., 2012). The river was diverted to the Harper basin at least twice during the late Pleistocene based on deposits in Hinkley Valley and Harper basin (Meek, 1999; Garcia et al., 2014; Miller et al., 2020;). The current divide between the Mojave River and Harper Lake is low enough that the river could have historically diverted to Harper Lake during major floods as suggested by anecdotal accounts (Miller et al., 2020). However, the nearly continuous sedimentation record preserved in the Manix basin from about 340–25 ka, broken only by apparently relatively brief soil-forming intervals, suggests that any diversions into Harper basin must have been short-lived (Reheis et al., 2012).

Well logs examined for this study suggest that prior to arrival of the river, parts of the basin floor near Yermo were 10–30 m deeper than the basin floor near Manix Wash (Fig. 4). These relations suggest that lacustrine deposition may not have occurred in the Manix Wash area early in lake history until there were no lower areas in the basin floor, or until this deeper area was partly filled in by a clastic wedge. In addition, they imply that early in lake history, clastic deposits were localized in this western area. The clastic wedge and its delta component total an estimated 5.5 km^3, of which more than half contributed to the reduction of accommodation space below highstand levels of Lake Manix.

Near the confluence of Manix Wash and the Mojave River, the stratigraphic section below the 184-ka Manix tephra is as much as 24 m thick (Ql1–Ql5) and consists mainly of alternating lacustrine muds and minor amounts of locally derived distal fan sediments. Thus, considerable accommodation space was filled at this location during the early part of Lake Manix history, even though the sediments do not indicate proximity to a delta. Using an approximate age of 480 ka for the base of the Manix core (Reheis et al., 2012), the accumulation rate in this area, which was not the depocenter for much of this time, was ~0.08 m/kyr. After tephra deposition at ~184 ka, the accumulation rate increased to >0.1 m/kyr and the sediment became coarser grained as the Mojave River delta prograded toward the confluence.

In the Afton subbasin, the initial influx of Ql6 sediment derived from the Cady subbasin upstream was extremely rapid. Assuming the onset of Ql6 occurred at about 190 ka, before deposition of the Manix tephra, and ended before basal tufa ages on Ql7 (Table 3) of ~180 ka, the deposition rate was at least 1.0 m/kyr in the clastic wedge southwest of Dunn wash (Figs. 7, 8, 9). For Ql7 in the Dunn Island section, assuming deposition ended well before the basal ^{14}C and tufa ages on Ql8 deposits of about 50 ka, minimum accumulation rates were 0.3 m/kyr.

Average accumulation rates therefore appear to have increased downstream through time. In the Victorville basin upstream, in which the river terminated from before ~2.5 Ma to after 760 ka, average accumulation rates near the basin center increased from 0.04 to 0.07 m/kyr (60 and 78 m thick, respectively; Cox et al., 2003). In the Cady subbasin of Lake Manix between ~480 and 25 ka (~45 m thick), rates increased from at least 0.08 to >0.1 m/kyr, and in the Afton subbasin between 180 and 25 ka (~20–30 m thick), rates were 0.3–0.7 m/kyr. In Lake Mojave downstream of Lake Manix, in which the river terminated much of the time from about 26–8 ka, average accumulation rates were ~1–2 m/kyr in the Soda Lake subbasin (25 m thick) and 1 m/kyr in the Silver Lake subbasin (calculated using data in Wells et al., 2003, and Honke et al., 2019). The increasing rates through time in a given basin are not easily explained by the Sadler (1981) effect whereby younger sediments are thicker because they are better preserved or span shorter periods of time, because the downstream basin captures and subsequent incision by the Mojave River and its tributaries have caused erosion and thinning of the youngest sediments in the Cady and Afton areas. The increase within a basin is likely caused by a combination of factors including ongoing uplift of the source area in the Transverse Ranges and encroachment of the fluvial delta in some places. The downstream increase in apparent accumulation rate from basin to basin is most likely caused by increasing availability of easily eroded sediment from previously filled basins that, in their turn, became source areas.

5.2. Cady-Afton integration and a catastrophic flood

The most significant event in the history of Lake Manix was the integration of the Afton subbasin (Fig. 2). The sequence of exposed lake deposits clearly indicates that lake water did not enter this subbasin until shortly before deposition of the Manix tephra at ~184 ka (Figs. 4, 5, 8) during Ql6 time. The integration event had two important consequences for subsequent basin history: (1) the lake was able to expand over a larger area, thus increasing evaporation volumes and acting to stabilize lake level; and (2) because much of the volume of the upstream subbasins had been filled with sediment and the Afton subbasin was lower in elevation and held a large volume of water, relatively high lake levels were required to submerge areas such as that near Manix Wash where sediment had filled much of the accommodation space. Thus, the sedimentary record of Ql7 in the Cady subbasin is largely one of mudflat and fluvial deposits interspersed with relatively shallow-water lacustrine silt and sand and less commonly, deeper-water muds (Reheis et al., 2012), whereas Ql7 in lower parts of the Afton subbasin is dominated by deep-water mud. In addition, as the fluvial delta prograded eastward and encroached on the sill that lay near Buwalda Ridge, the sill was an effective barrier to delta sediments, thereby reducing the sedimentation rates in the Afton basin markedly. Below, we summarize the evidence for a catastrophic flood and subsequent effects of integration on the two subbasins. The sequence of events was reconstructed from many measured sections (Figs. 5 and 8; Reheis et al., 2014b) and is summarized in Figs. 9 and 10.

Fluvial deposits within Ql6 in the Afton subbasin (Fig. 7) document a catastrophic flood that initiated integration of this subbasin. At several sites near the formerly deepest part of the subbasin (near Dunn wash), these fluvial deposits contain several meters of chaotically bedded blocks (as much as 2 m across) of semi-indurated green lake mud, silt, and sand mixed with brown playa mud (Figs. 6D–E and 8). The blocks of lake sediment retain internal bedding that is commonly deformed; the bedding orientation varies among blocks. Similar, smaller clasts of reworked lake sediment are incorporated into the fluvial strata. At one site on the southeastern flank of Buwalda Ridge (M09-127, Fig. 6B), crossbedded fluvial deposits rest on a steeply sloping buttress unconformity cut on older, indurated, poorly sorted fan deposits. The fluvial deposits grade upslope into a chaotic mass of poorly sorted sand and gravel that contains scattered lumps of green lake sediment, suggesting that sediment eroded from the older fan deposits was mixed with flood-transported mud lumps and plastered against the valley wall. We interpret these relations to record a sudden failure of the sill between Cady and Afton subbasins that triggered a flood of lake water, which quarried and transported lake sediment from the Cady subbasin and sand and gravel derived from the flank of Buwalda Ridge (Figs. 4 and 7). This flood may have occurred partly as a fluidized mudflow, because it seems improbable that the large, weakly consolidated blocks of lake sediment found in central Afton subbasin could have

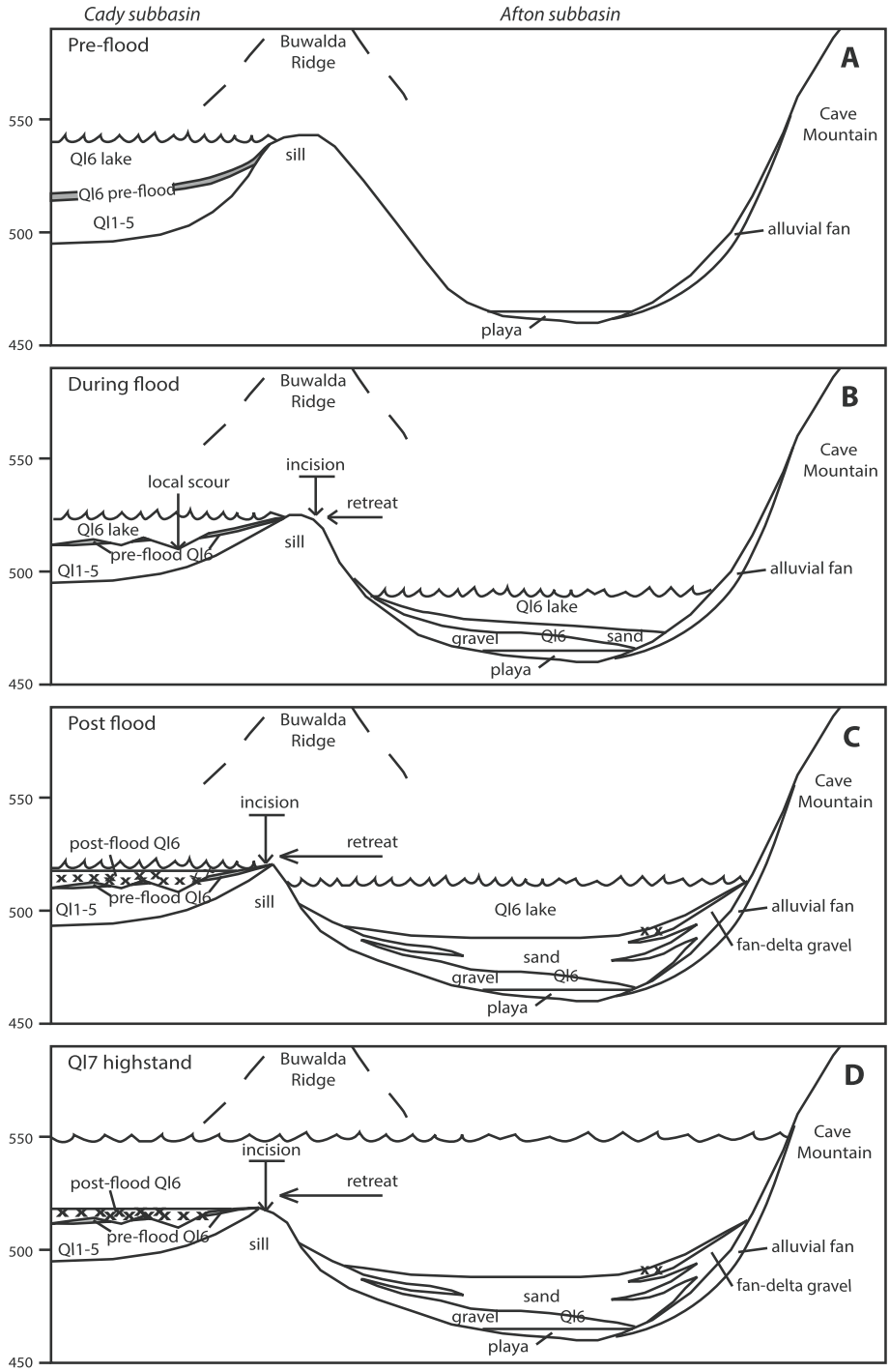

Fig. 10. Schematic history of events related to failure of Buwalda Ridge sill between the Cady and Afton subbasins and subsequent incision. (A) "Pre-flood" depicts rise of Ql6 lake to a sill at about 542 masl in the Cady subbasin, and a dry playa in the Afton subbasin. (B) During flood, sill is rapidly incised and eroded while lake deposits in the Cady subbasin are locally scoured (the rip-up beds); downstream, flood beds are superseded by rapid aggradation of gravel and sand. (C) After the flood, lake level temporarily stabilized at two different elevations separated by a remnant of the sill, and lacustrine sediments containing the Manix tephra (X's in diagram) were deposited. (D) During the following Ql7 phase, the lake level would first have risen to the level of the former sill, then spilled into and filled the Afton subbasin, subsequently rising to perhaps as high as 550 masl. The sill may have been entirely eroded during this episode or persisted longer.

been transported at least 7 km as bedload without being completely disaggregated.

The sudden drop in lake level upstream must have caused erosion and slope failure, evidence for which is preserved at many sites in the Cady subbasin within Ql6 deposits (Fig. 5). At these sites, for example M10-11 and JO-14 in Manix Wash and M09-58, -66, and -76 south of the river, basal, fine-grained Ql6 sediment records an initial rise of the lake that is abruptly overlain by contorted beds with brecciated mud or rip-ups of green mud within unsorted gravel and sand (Fig. 6A, C). These contorted beds are interpreted to represent remobilization of unconsolidated sediment as the lake dropped. At higher elevations, the contorted beds are typically capped by a buried soil and then by Ql7 deposits, whereas at elevations between about 514 and 522 m, the contorted beds are overlain by lacustrine sand and silt, commonly containing the Manix tephra. At yet lower elevations that were then deeper in the lake, no rip-ups or other disturbances appear below the tephra.

The maximum elevations of Ql6 sediment in the two subbasins are different (Table 4; Fig. 9). In the Cady subbasin, pre-flood Ql6 deposits extend as high as 541 masl, but only to 522 masl in post-flood deposits containing the Manix tephra. In the Afton subbasin, post-flood Ql6 deposits extend only as high as 513 masl. We interpret these relations to suggest that the sill on the flank of Buwalda Ridge was not entirely removed during Ql6 time so that the lake levels in the two subbasins did not equalize.

These rather complicated relations can be envisioned as a time sequence of events reconstructed from the distribution of lake and fluvial sediments (Fig. 10). Prior to integration, probably during the earliest part of MIS 6, Lake Manix began to rise, and reached an elevation of about 541 m (Fig. 10A). It may have stabilized at that level temporarily, because this is also the approximate elevation of the bedrock sill between the Cady and Coyote subbasins. Overflow at, and subsequent catastrophic failure of, the sill at Buwalda Ridge caused rapid incision of the sill and adjacent lacustrine deposits and consequent aggradation of gravel, sand, and finer sediment in the Afton subbasin (Fig. 10B). As water level rose in the Afton subbasin, the hydraulic gradient decreased and the rate of sill incision likely slowed; eventually, the Ql6 lakes stabilized at different elevations in the two subbasins, separated by about 10 m of elevation (Fig. 10C). Presumably, at this time a stable short river flowed from the Cady to the Afton subbasin. Lake level in both basins then dropped and a brief hiatus marked by a buried soil in both subbasins ensued. During the next lake rise at the beginning of Ql7 time, the lake would first have filled the Cady subbasin to the top of the eroded sill at about 522 masl and then overflowed into the Afton subbasin. This scenario implies a second influx of fluvial sediment just downstream of the sill, and a few measured sections in this area do suggest that the basal Ql7 sediment is partly fluvial in character (Reheis et al., 2014b). Eventually, the two lakes merged at a single level (Fig. 10D).

Two interesting questions remain in this reconstructed scenario. First, did the eroded sill persist through the following lacustrine history of Ql7 and Ql8, or was it entirely incised during Ql7 time? The Mojave River has since incised through the sill area, which likely lay at a north-pointing projection of the older Cady Mountains fan gravels near the eastern end of Buwalda Ridge (Fig. 2). A small knickpoint is located where the stream gradient increases from about 0.4% to 0.7% slope at about 34.98°, −116.52°, in the area of this projection. In addition, the projection has a nearly flat beveled surface, thinly covered with fluvial sediment (BS, Fig. 7), almost a kilometer long between 519 and 524 masl, which is approximately the elevation of the reconstructed sill at the end of Ql6 time. This surface might represent a remnant of this sill that was later incised when the Afton sill was cut, and the river then flowed to the Lake Mojave basin farther downstream. The beveled area suggests that the sill may have persisted into early Ql7 time, but there is no evidence to support either its persistence or removal after that time.

Second, such an integration event must have removed considerable lake sediment from the Cady subbasin near the sill and likely would have cut a channel westward into the sediment. Where did that channel lie? An easy option would be that the channel was cut in the same position as the modern Mojave River channel (Figs. 2 and 4). This may be true for the reach immediately west of the former sill, which is confined on the north by Buwalda Ridge and on the south by high-standing remnants of Cady Mountains fan gravel and deposits of the Mojave River formation that lie within an abandoned meander. However, the modern river jogs sharply south near the confluence of Manix Wash and resumes an easterly course after turning a hairpin bend. Exposures are generally excellent along these southern and western reaches, yet we have observed no evidence for erosion of pre-Ql6 sediment suggesting the presence of a channel incised during the integration event.

An alternative channel is suggested by outcrops about 1 km directly west of the confluence of the Mojave River and Manix Wash. Sites in this area preserve sand, likely fluvial, as much as 2–3 m thick filling a paleochannel incised into Ql5 and older sediment; the sand is overlain by mudflat to shallow-lacustrine Ql6 deposits containing lenticular pods of the Manix tephra, in turn overlain by Ql7 deposits. Interestingly, this course approximately coincides with an abandoned channel carved into deltaic sands of unit Ql8 during early incision caused by the late Pleistocene failure of the Afton sill (Reheis et al., 2007). The lowest elevation of the base of the older paleochannel is about 520 masl (from lidar data), slightly lower than the elevation of the post-flood remnant sill (Figs. 9 and 10). Thus, if this paleochannel does mark erosion associated with the integration event, it may represent over-deepening, perhaps caused by turbulent currents induced by the sill failure. Alternatively, the elevations may have been altered by deformation along the Manix fault, multiple strands of which parallel or coincide with the reach west of the Buwalda sill (Fig. 4; Reheis et al., 2014b).

5.3. Effects of Manix fault and earthquakes

The history of Lake Manix has been strongly influenced by regional tectonics associated with the left-lateral Manix fault and interconnected faults of the Eastern California shear zone (Fig. 2; McGill et al., 1988; Miller and Yount, 2002; Reheis et al., 2007). The Cady and Afton subbasins lie atop or adjacent to strands of the Manix fault zone, which underlies both the Buwalda Ridge and Afton Canyon paleo-sills. These subbasins lie in a trough that has occupied areas north of the Manix fault at least since the early Pliocene (Miller et al., 2011). The trough has lain farther north much of this time but shifted to the present position by the beginning of Mojave River formation deposition ~2 Ma. Meek (2015) argued that relative uplift of the Cady Mountains to create the Afton subbasin did not begin until the early to middle Pleistocene. However, playa deposits that lie beneath Ql6 flood deposits (site M06-100, Figs. 6D, 7, 8) and older playa deposits east of Buwalda Ridge (Reheis et al., 2014b) demonstrate the presence of at least a shallow basin during the Pleistocene in the approximate position of the modern basin.

Water-well records in the basin demonstrate that bedrock is uplifted in places along the Calico fault, but the effects on Lake Manix are not clear. Lake sediments and older rocks have been uplifted along the western part of the Manix fault and parts of the Dolores Lake fault (Fig. 4), probably decreasing the accommodation space for Lake Manix in minor ways. Farther east, where lake sediments are better preserved and have been extensively studied, the effects of faults are clearer. In the eastern Cady subbasin (Fig. 4), minor north-striking normal faults parallel the north-trending reach of the Mojave River hairpin and likely controlled thickness of lake-sediment deposition east of this reach. These normal faults and others northeast of Buwalda Ridge displace Ql7 and older units, but not the younger Ql8 deposits. Strands of the Manix fault cut all ages of exposed lake deposits and older sediment in the vicinity of Manix Wash and Buwalda Ridge (McGill et al., 1988; Reheis et al., 2014b). Strike-slip displacements are identifiable by abrupt cross-fault thickness or facies changes of lake units and by shear zones with subhorizontal slickenlines. Near the Manix and nearby faults in the Afton subbasin, Ql8 deposits either have largely been eroded or were not deposited, but Ql8 and even younger fan deposits are displaced in a few locations.

Lake Manix sediments locally display soft-sediment deformation that may have been caused by earthquakes that occurred during lake cycles. Such evidence ranges from faults to contorted bedding to sand blows (Fig. 11). Of the 21 triggers summarized by Shanmugam (2016) in a review of "seismites," only three could apply to the Manix area: earthquake, sediment loading, and mass movement. In the delta area or along steep lake margins, contorted beds could have been caused by sediment loading or slope failure. However, most of the lake margins are alluvial fans with relatively low gradients, and the contorted beds commonly are found far from the Mojave River delta and lake margins. One stratigraphic interval containing evidence for possible earthquake disturbance lies near the base of the upper Ql7 unit in the Afton subbasin. In several widely spaced locations, these features include brecciated muds, clay and sand diapirs, and wavy distorted bedding (Table 1; Fig. 11) that are not observed

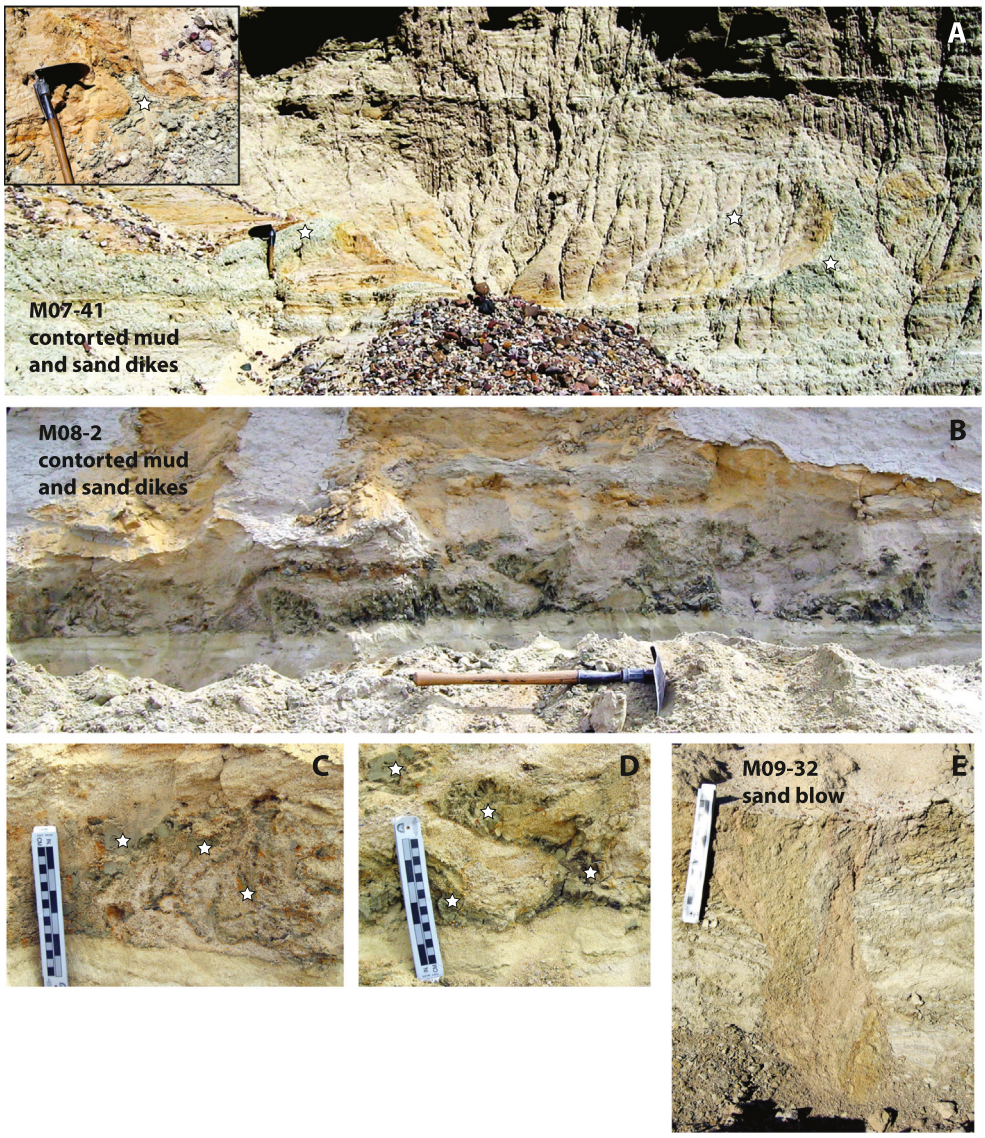

Fig. 11. Photographs of earthquake deformation (locations on Table 1 and Figs. 4 and 7). Stars show contorted beds of green mud. A and B, contorted mud and sand dikes just above the Ql7a-Ql7b contact in the Afton subbasin. Shovel is ~50 cm long. C and D, close-ups of contortions in B. E, Sand blow cutting sediments of Ql7 in the Cady subbasin. Scale is 15 cm long. All photos by M. Reheis.

elsewhere in unit Ql7. Similar distortion was noted by Meek (1990) above a hiatus in Ql7 marked by oxidized coarse sand, in a measured section south of the river adjacent to a strand of the Manix fault. Another possible event is recorded by several outcrops near the Manix fault on the west side of Manix Wash. These exhibit sand blows that terminate upward at the top of unit Ql7 (Fig. 11E). A similar sand blow was observed to the north in basal Ql8 sediment.

To attribute the failures of the Buwalda Ridge and Afton sills to earthquake events is tempting, because both these sills lay athwart the Manix fault zone (Figs. 2, 4, and 7). However, we lack direct evidence of such events. Incision of the sill at the head of Afton Canyon (Figs. 2 and 4) effectively terminated lacustrine deposition in the Cady and Afton subbasins, although the lake may have episodically discharged over the sill before rapid incision began (Reheis and Redwine, 2008). In the case of the Buwalda sill, disturbance in the pre-flood lake sediment caused by the sudden drop in base level obscured possible earthquake evidence, although fractures with millimeter-scale displacement are present in the core below the Manix tephra. It seems just as likely that intense shearing in Tertiary conglomerates cut by the Manix fault zone may have preconditioned these two sills to fail by knickpoint retreat of a tributary or by groundwater sapping, as well as being the location of significant topographic saddles of poorly resistant broken rock.

In summary, the role of tectonic activity in the Manix basin largely has been to control (1) the configuration of the subbasins through development of structural depressions and (2) the failure of interbasin sills through shearing of underlying fan deposits.

5.4. Effects of climate change

Glacial-interglacial climate change has played a major role in the history of Lake Manix. Its effect on the geomorphic evolution of the basin has been more subtle, expressed mainly as rate of sediment delivery by the Mojave River and as a control on the timing of greatly increased discharge and frequency of floods that may correlate with drainage integration events. We briefly summarize here the history of climate change recorded by Lake Manix sediments, details of which are the subject of other papers (Reheis et al., 2012, 2015).

Lake Manix sediments provide a robust record of Mojave River discharge over the last half-million years, but do not correlate solely with glacial climates as indicated for basins farther north (e.g., Smith et al., 1997; Oviatt et al., 1999; Reheis et al., 2002a). Lakes have inundated the Cady

and Afton subbasins repeatedly and consistently from MIS 12 through early MIS 2 (Reheis et al., 2012, 2015). The Manix core record indicates that from ~400 to 190 ka, sedimentation was nearly continuous in the Cady subbasin, with only five brief hiatuses marked by desiccation surfaces and oxidized vertisols, which can form very quickly in clay-rich sediment (Birkeland, 1999). This part of Lake Manix appears to have maintained shallow to moderate water depths during most of interglacial MIS 7 and probably 9, as well as relatively deep lakes during glacial MIS 10, 8, and 6. Assuming that river discharge is correlated with sediment transport and deposition, it seems likely that deposition rates were faster during full-lake conditions. However, the presence of shallow to moderately deep lakes during interglacial periods indicates that sediment transport and deposition did not cease altogether except when the lake desiccated.

Full-lake conditions were probably a prerequisite for drainage integration events and were also necessary for full connectivity over the Coyote-Cady subbasin sill (Fig. 2). Increasing depth and volume of lake water would tend to increase the hydrologic head above an adjacent dry subbasin, and would increase the likelihood of groundwater leakage, leading to sapping or piping through the faulted sediments that formed the Buwalda and Afton sills. The pre-flood, pre-tephra Ql6 deposits in Cady subbasin are preserved up to about 541 m elevation, which suggests that increased discharge at the beginning of glacial MIS 6, about 190 ka (Lisiecki and Raymo, 2005), led to rapid lake rise in a subbasin already partly filled with older sediment, leading to consequent failure of the Buwalda sill. A similar rapid rise may have led to incision of the Afton sill early in MIS 2, in this case preceded by several lake highstands during interstadial MIS 3 that reached or even briefly overflowed the sill (Reheis and Redwine, 2008; Reheis et al., 2015).

6. Conclusions

The Lake Manix basin preserves a half-million-year record of geomorphic, climatic, and tectonic events recorded by lacustrine and alluvial deposits. This record is conditioned by the multiple basins in which the Mojave River sometimes terminated (Meek, 1994, 1999; Cox et al., 2003; Enzel et al., 2003; Miller et al., 2020), at times behaving rather like a firehose with no one to direct the nozzle. We employed outcrop studies of incised basin fill coupled with a 45-m core (Reheis et al., 2012) to reconstruct this history, provide constraints on absolute lake level and rate of sediment infilling, and understand the dramatic changes caused by the catastrophic integration of two subbasins.

The Mojave River entered the Manix basin before 480 ka, perhaps ~500 ka. During the earliest part of Lake Manix history, the deepest part of the lake basin was probably near Yermo (Fig. 4), but rapid progradation of a clastic wedge filled this subbasin. Until about 190 ka, Lake Manix was confined to the Cady-Troy and Coyote subbasins and fluctuated in response to climate change and likely also to brief diversions of the river into the Harper Lake basin. At times, the river flowed directly into the Coyote subbasin to the north (Miller et al., 2019). Nevertheless, the record preserved in the Manix core indicates nearly continuous lacustrine deposition in the Cady subbasin from ~400 to 190 ka (Reheis et al., 2012). During this time, about 19 m of mainly deeper water sediment accumulated near the confluence of the Mojave River and Manix Wash, gradually filling the accommodation space. After sill failure, the core and outcrop sediments instead record periods of shallow water, mudflats, and desiccation, followed by fluvial-deltaic conditions.

When the lake began to rise at the onset of glacial MIS 6 (~190 ka), it overtopped the sill on the south flank of Buwalda Ridge, triggering sill failure (possibly preconditioned by sapping through sheared fan deposits underlying the sill) and a catastrophic flood. The flood eroded blocks of older lake sediment and rafted them downstream to the playa floor of Afton subbasin, where they were rapidly buried by gravel and sand eroded from the Buwalda Ridge area. The bottom sediments upstream of the sill were destabilized by the sudden drop in lake level. As water rose in the topographically lower Afton subbasin, the hydraulic head decreased and lake level temporarily stabilized at different levels in the two subbasins, allowing deposition of quiet-water sediments, during which 184-ka Manix tephra was deposited. Subsequent MIS 6–2 lake-level changes (~190–25 ka) are recorded at similar elevations in both subbasins. The thickest deposits of this period are preserved in the Afton subbasin, and the area near the confluence of the Mojave River and Manix Wash was only submerged during relatively high lake levels. Thus, sediment records discussed here partly reflect response to geomorphic events (basin integration) rather than to fluctuating climatic conditions.

The hydrographic sill of Lake Manix after the integration event shifted to the northeast end of the Afton subbasin, athwart strands of the Manix fault zone. It is likely that this sill initially lay at about 550–558 masl (Reheis et al., 2014b) but was gradually incised to about 543 masl. At about 25 ka, this easternmost sill also failed, and the Mojave River advanced to terminate in Lake Mojave in Soda and Silver Lake basins (Wells et al., 2003). Whether this rapid incision was catastrophic, like that of the failure recorded by the flood deposits in Afton subbasin, is unknown because of deep burial by post-incision sediments at the mouth of Afton Canyon (Meek, 1989a, 1989b).

Are such sequential lake-overflow histories a common occurrence in integrating fluvial drainage systems? An active tectonic regime is presumably required to set the stage as in the case in the Basin and Range province of the western U.S. and many other extensional regimes. Another prerequisite, particularly in arid climates, is sufficient uplift to create high topography, inducing orographic precipitation and becoming a source area for stream drainage. A third factor is that rates of faulting must be slow enough that uplift is slower than basin sedimentation; if uplift is too rapid, basins will remain isolated. Basin integration by lake overflow has occurred numerous times in several different areas of the Basin and Range (Gale, 1914; Bachhuber, 1989; Bouchard et al., 1998; Sack, 2002; Reheis et al., 2003; Machette et al., 2007; Menges, 2008; Phillips, 2008), in the Altiplano of South America (Placzek et al., 2006), in Spain (Garcia-Castellanos et al., 2003), and has even been proposed for the early history of Mars (Rossman and Howard, 2002). Recognition of catastrophic floods as a driver of basin integration is less common, in part because of burial of the downstream evidence. However, in addition to Lake Manix, such floods have been documented for the Lake Russell-Lake Adobe system (Mono Lake to Owens River, California; Reheis et al., 2002b), the Lake Alvord-Lake Coyote system (Alvord basin to Owyhee River, Oregon; Carter et al., 2006), and the Colorado River below Grand Canyon (Meek and Douglass, 2001; House et al., 2008). Regardless of rate, integration events are significant in the evolution of lake basins. Recognition and dating of integration events are important to (1) provide the correct context for interpreting paleoclimate records from sediments and (2) provide temporal and spatial constraints on hydrologic connections that affected the biogeography of aquatic species (e.g., Hubbs and Miller, 1948; Smith et al., 2002; Hershler and Liu, 2008).

Declaration of competing interest

The authors declare that they have no known competing financial interests or personal relationships that could have appeared to influence the work reported in this paper.

Acknowledgements

Our work has benefited from many discussions in the field with George Jefferson and Norman Meek, and Michael Rosen provided insights on tufa growth. John McGeehin (U.S. Geological Survey) provided the many radiocarbon ages. Stephanie Dudash contributed to field mapping in the Coyote subbasin. We are grateful for the help of Anna Garcia of the Mojave Water Agency, who provided well logs, and David Buesch for help with interpreting logs. We thank the many field assistants who helped with field work. We appreciate the helpful comments of W.

Geoffrey Spaulding, Norman Meek, Adam Hudson, and two anonymous reviewers. This study was supported by funding from the National Cooperative Geologic Mapping Program and the Climate Program of the U.S. Geological Survey. Any use of trade, firm, or product names is for descriptive purposes only and does not imply endorsement by the U.S. Government.

Appendix A. Supplementary data

Supplementary data to this article can be found online at https://doi.org/10.1016/j.geomorph.2021.107901.

References

Adams, K.D., 2007. Late Holocene sedimentary environments and lake-level fluctuations at Walker Lake, Nevada, USA. Geol. Soc. Am. Bull. 119, 126–139.

Allen, B.D., Anderson, R.Y., 2000. A continuous, high-resolution record of late Pleistocene climate variability from the Estancia basin, New Mexico. Geol. Soc. Am. Bull. 112, 1444–1458.

Anderson, D.E., Wells, S.G., 2003. Latest Pleistocene highstands in Death Valley, California. In: Enzel, Y., Wells, S.G., Lancaster, N. (Eds.), Paleoenvironments and Paleohydrology of the Mojave and Southern Great Basin Deserts. Geological Society of America Special Paper 368, pp. 115–128.

Awramik, S.M., Bucheim, H.P., Leggitt, L., Woo, K.S., 2000. Oncoids of the late Pleistocene Manix Formation, Mojave Desert region, California. In: Reynolds, R.E., Reynolds, A.C. (Eds.), Empty Basins, Vanished Lakes. San Bernardino County Museum Quarterly Vol. 47(2), pp. 25–31.

Bachhuber, F.W., 1989. The occurrence and paleolimnologic significance of cutthroat trout (*Oncorhynchus clarki*) in pluvial lakes of the Estancia Valley, central New Mexico. Geol. Soc. Am. Bull. 101, 1543–1551.

Benson, L., 2004. Western lakes. In: Gillespie, A.R., Porter, S.C., Atwater, B.F. (Eds.), The Quaternary Period in the United States. Elsevier, New York, pp. 185–204.

Benson, L., Kashgarian, M., Rye, R., Lund, S., Paillet, F., Smoot, J., Kester, C., Mensing, S., Meko, D., Lindstrom, S., 2002. Holocene multidecadal and multicentennial droughts affecting northern California and Nevada. Quat. Sci. Rev. 21, 659–682.

Benson, L.V., Burdett, J.W., Kashgarian, M., Lund, S.P., Phillips, F.M., Rye, R.O., 1996. Climatic and hydrologic oscillations in the Owens Lake basin and the adjacent Sierra Nevada, California. Science 274, 746–749.

Benson, L.V., Lund, S.P., Smoot, J.P., Rhode, D.E., Spencer, R.J., Verosub, K.L., Louderback, L.A., Johnson, C.A., Rye, R.O., Negrini, R.M., 2011. The rise and fall of Lake Bonneville between 45 and 10.5 ka. Quat. Int. 235, 57–69.

Birkeland, P.W., 1999. Soils and Geomorphology. Oxford University Press, New York 430 p.

Bischoff, J.L., Fitzpatrick, J.A., 1991. U-series dating of impure carbonates: an isochron technique using total-sample dissolution. Geochim. Cosmochim. Acta 55, 543–554. https://doi.org/10.1016/0016-7037(91)90011-S.

Bischoff, J.L., Menking, K.M., Fitts, J.P., Fitzpatrick, J.A., 1997. Climatic oscillations 10,000–155,000 yr B.P. at Owens Lake, California reflected in glacial rock flour abundance and lake salinity in Core OL-92. Quat. Res. 48, 313–325.

Blackwelder, E., Ellsworth, E.W., 1936. Pleistocene lakes of the Afton basin, California. Am. J. Sci. 231, 453–463.

Blaney, F.H., 1957. Evaporation study at Silver Lake in the Mojave Desert, California. Eos 38, 209–215.

Bortugno, E.J., Spittler, T.E., 1986. Geologic Map of California, San Bernardino Sheet. Department of Conservation, California Division of Mines and Geology (scale 1: 250,000).

Bouchard, D.P., Kaufman, D.S., Hochberg, A., Quade, J., 1998. Quaternary history of the Thatcher Basin, Idaho, reconstructed from the $^{87}Sr/^{86}Sr$ and amino acid composition of lacustrine fossils: implications for the diversion of the Bear River into the Bonneville Basin. Paleogeogr. Paleoclimatol. Palaeoecol. 141, 95–114.

Buwalda, J.P., 1914. Pleistocene beds at Manix in the eastern Mohave Desert region. Univ. Cal. Publ. Geol. Sci. 7 (24), 443–464.

Byers Jr., F.M., 1960. Geology of the Alvord Mountain quadrangle, San Bernardino County, California. U.S. Geol. Surv. Bull. 1089-A 71 p.

Cameron, S.P., 1971. Ostracodes of Pluvial Lake Cochise, Cochise County, Arizona. M.S. Thesis. Arizona State University, Tempe, Arizona 65 p.

Carter, D.T., Ely, L.L., O'Connor, J.E., Fenton, C.R., 2006. Late Pleistocene outburst flooding from pluvial Lake Alvord into the Owyhee River, Oregon. Geomorphology 75, 346–367.

Cheng, H., Edwards, R.L., Shen, C.C., Polyak, V.J., Asmerom, Y., Woodhead, J., Hellstrom, J., Wang, Y., Kong, X., Spötl, C., Wang, X., Alexander Jr., E.C., 2013. Improvements in ^{230}Th dating, ^{230}Th and ^{234}U half-life values, and U–Th isotopic measurements by multi-collector inductively coupledplasma mass spectrometry. Earth Planet. Sci. Lett. 371-372, 82–91. https://doi.org/10.1016/j.epsl.2013.04.006.

Cox, B.F., Hillhouse, J.W., Owen, L.A., 2003. Pliocene and Pleistocene evolution of the Mojave River, and associated tectonic development of the Transverse Ranges and Mojave Desert, based on borehole stratigraphy studies and mapping of landforms and sediments near Victorville, California. In: Enzel, Y., Wells, S.G., Lancaster, N. (Eds.), Paleoenvironments and Paleohydrology of the Mojave and Southern Great Basin Deserts. Geological Society of America Special Paper 368, pp. 1–42.

Danehy, E.A., Collier, J.T., 1958. Area economic geology map of T. 11N, R. 5 & 6 E. Southern Pacific Mineral Survey, Scale 1:24,000.

Delorme, L.D., 1967. New freshwater Ostracoda from Saskatchewan, Canada. Can. J. Zool. 45, 357–363. https://doi.org/10.1139/z67-047.

Delorme, L.D., 1971. Freshwater ostracodes of Canada. Part V. Families Limnocytheriae, Loxoconchidae. Can. J. Zool. 49, 43–64.

Denison-Budak, C.W., 2010. Ostracodes as Indicators of the Paleoenvironment in the Pliocene Glenns Ferry Formation, Glenns Ferry Lake, Idaho. M.S. Thesis. Kent State University, Kent, Ohio 118 p.

Densmore, J.N., Cox, B.F., Crawford, S.M., 1996. Geohydrology and water quality of Marine Corps logistics base, Nebo and Yermo Annexes, near Barstow, California. U.S. Geol. Surv. Water-Resour. Investig. Rep. 96-4301 116 p.

Dibblee Jr., T.W., 1968. Geology of the Opal Mountain and Fremont Peak quadrangles, California. Cal. Div. Mines Geol. Bull. 188 64 p.

Dokka, R.K., Travis, C.J., 1990. The eastern California shear zone and its role in the tectonic evolution of the Pacific-North American transform boundary. Geol. Soc. Am. Abstr. Progr. 22 (3), 19.

Dudash, S.L., 2006. Preliminary surficial geologic map of a Calico Mountains piedmont and part of Coyote Lake, Mojave Desert, San Bernardino County, California. U.S. Geol. Surv. Open-File Rep. 2006–1090 44 p., scale 1:24,000.

Ellsworth, E.W., 1932. Physiographic History of the Afton Basin. [Ph.D. thesis]. Stanford University, Palo Alto 99 p.

Enzel, Y., 1992. Flood frequency of the Mojave River and formation of late Holocene playa lakes, southern California, USA. Holocene 2, 11–18.

Enzel, Y., Wells, S.G., 1997. Extracting Holocene paleohydrology and paleoclimatology information from modern extreme flood events: an example from southern California. Geomorphology 19, 203–226.

Enzel, Y., Wells, S.G., Lancaster, N., 2003. Late Pleistocene lakes along the Mojave River, southeast California. In: Enzel, Y., Wells, S.G., Lancaster, N. (Eds.), Paleoenvironments and Paleohydrology of the Mojave and Southern Great Basin Deserts. Geological Society of America Special Paper 368, pp. 61–77.

Forester, R.M., 1985. *Limnocythere bradburyi* n. sp.: a modern ostracode from central Mexico and a possible Quaternary paleoclimate indicator. J. Paleontol. 59, 8–20.

Forester, R.M., 1988. Nonmarine calcareous microfossil sample preparation and data acquisition procedures. U.S. Geological Survey Technical Procedure HP-78 R1 (9 p).

Forester, R.M., Bradbury, P.J., 1981. The paleoenvironmental implications of the ostracodes and diatoms from selected samples in Pliocene and Pleistocene lacustrine sediments in the Beaver Basin, Utah. U.S. Geol. Surv. Open File Rep. 81-390 55 p.

Forester, R.M., Lowenstein, T.K., Spencer, R.J., 2005a. An ostracode based paleolimnologic and paleohydrologic history of Death Valley: 200 to 0 ka. Geol. Soc. Am. Bull. 117, 1379–1386.

Forester, R.M., Smith, A.J., Palmer, D.F., Curry, B.B., 2005b. North American non-marine ostracode database project, v. 1. http://www.personal.kent.edu/~alisonjs/nanaode/index.htm.

Gale, H.S., 1914. Salines in the Owens, Searles, and Panamint Basins, southeastern California. U.S. Geol. Surv. Bull. 580-L, 251–323.

Garcia, A.L., Knott, J.R., Mahan, S.A., Bright, J., 2014. Geochronology and paleoenvironment of pluvial Harper Lake, Mojave Desert, California, USA. Quat. Res. 81, 305–317.

Garcia-Castellanos, D., Verges, J., Gaspar-Escribano, J., Cloetingh, S., 2003. Interplay between tectonics, climate, and fluvial transport during the Cenozoic evolution of the Ebro Basin (NE Iberia). J. Geophys. Res. 108. https://doi.org/10.1029/2002JB002073 8 p.

Goudie, A.S., 1983. Calcrete. In: Goudie, A.S., Pye, K. (Eds.), Chemical Sediments and Geomorphology: Precipitates and Residua in the Near-surface Environment. Academic Press, New York, pp. 93–131.

Groat, C.G., 1967. Geology and Hydrology of the Troy Playa Area, San Bernardino County, CA. M.S. thesis. University of Massachusetts, Amherst 133 p.

Hagar, D.J., 1966. Geomorphology of Coyote Valley, San Bernardino County, California. Ph. D. thesis. University of Massachusetts, Amherst, MA 210 p.

Hershler, R., Liu, H.-P., 2008. Ancient vicariance and recent dispersal of springsnails (Hydrobiidae: *Pyrgulopsis*) in the Death Valley system, California-Nevada. In: Reheis, M.C., Hershler, R., Miller, D.M. (Eds.), Late Cenozoic Drainage History of the Southwestern Great Basin and Lower Colorado River Region: Geologic and Biotic Perspectives. Geological Society of America Special Paper 43, pp. 91–101.

Honke, J.S., Pigati, J.S., Wilson, J., Bright, J., Goldstein, H.L., Skipp, G.L., Reheis, M.C., Havens, J.C., 2019. Late Quaternary paleohydrology of desert wetlands and pluvial lakes in the Soda Lake basin, central Mojave Desert, California (USA). Quat. Sci. Rev. 216, 89–106.

House, P.K., Pearthree, P.A., Perkins, M.E., 2008. Stratigraphic evidence for the role of lake spillover in the inception of the lower Colorado River in southern Nevada and western Arizona. In: Reheis, M.C., Hershler, R., Miller, D.M. (Eds.), Late Cenozoic Drainage History of the Great Basin and Lower Colorado River Region: Geologic and Biotic Perspectives. Geological Society of America Special Paper 439, pp. 335–353.

Hubbs, C.L., Miller, R.R., 1948. The Great Basin. II. The zoological evidence. Univ. Utah Bull. 38 (20), 17–166.

Jefferson, G.T., 1968. The Camp Cady Local Fauna from Pleistocene Lake Manix, California. M.S. thesis. University of California 106 p.

Jefferson, G.T., 1985. Stratigraphy and geologic history of the Pleistocene Manix Formation, central Mojave Desert, California. In: Reynolds, R.E. (Ed.), Geologic Investigations Along Interstate 15–Cajon Pass to Manix Lake, California: Field Trip Guidebook, Western Association of Vertebrate Paleontologists, Sixth Annual Meeting. San Bernardino County Museum, Redlands, pp. 157–169.

Jefferson, G.T., 2003. Stratigraphy and paleontology of the middle to late Pleistocene Manix Formation, and paleoenvironments of the central Mojave River, southern California. In: Enzel, Y., Wells, S.G. (Eds.), Paleoenvironments and Paleohydrology of the Mojave and Southern Great Basin Deserts. Geological Society of America Special Paper 368, pp. 43–60.

Kaufman, A., Broecker, W.S., 1965. Comparison of ^{230}Th and ^{14}C ages for carbonate materials from Lake Lahontan and Bonneville. J. Geophys. Res. 70, 4039–4054.

Kaufman, D.S., 2003. Amino acid paleothermometry of Quaternary ostracodes from the Bonneville Basin, Utah. Quat. Sci. Rev. 22, 899–914. https://doi.org/10.1016/S0277-3791(03)00006-4.
Kaufman, D.S., Manley, W.F., 1998. A new procedure for determining enantiometric (D/L) ratios in fossils using reverse phase liquid chromatography. Quat. Sci. Rev. (Quat. Geochronol.) 17, 98–100.
Kosnik, M.A., Kaufman, D.S., 2008. Identifying outliers and assessing the accuracy of amino acid racemization measurements for geochronology: II. Data screening. Quat. Geochronol. 3, 328–341. https://doi.org/10.1016/j.quatgeo.2008.04.001.
Ku, T.L., Luo, S., Lowenstein, T.K., Li, J., Spencer, R.J., 1998. U-series chronology of lacustrine deposits in Death Valley, California. Quat. Res. 50, 261–275.
Kurth, G., Phillips, F.M., Reheis, M.C., Redwine, J.L., Paces, J.B., 2011. Cosmogenic nuclide and uranium-series dating of old, high shorelines in the western Great Basin, USA. Geol. Soc. Am. Bull. 123, 744–768.
Lao, Y., Benson, L., 1988. Uranium-series age estimates and paleoclimatic significance of Pleistocene tufas from the Lahontan basin, California and Nevada. Quat. Res. 30, 165–176.
Lisiecki, L.E., Raymo, M.E., 2005. A Pliocene-Pleistocene stack of 57 globally distributed benthic $\delta^{18}O$ records. Paleoceanography 20 (PA1003). https://doi.org/10.1029/2004PA001071 17 p.
Lowenstein, T.K., Li, J., Brown, C., Roberts, S.M., Ku, T.-L., Luo, S., Yang, W., 1999. 200 k.y. paleoclimate record from Death Valley salt core. Geology 27, 3–6.
Ludwig, K.R., Paces, J.B., 2002. Uranium-series dating of pedogenic silica and carbonate, Crater Flat, Nevada. Geochim. Cosmochim. Acta 66, 487–506.
Machette, M.N., Marchetti, D.W., Thompson, R.A., 2007. Ancient Lake Alamosa and the Pliocene to middle Pleistocene evolution of the Rio Grande. In: Machette, M.N., Coates, M.-M., Johnson, M.L. (Eds.), 2007 Rocky Mountain Section Friends of the Pleistocene Field Trip—Quaternary Geology of the San Luis Basin of Colorado and New Mexico, September 7–9, 2007. U.S. Geological Survey Open-File Report 2007-1193, pp. 157–167.
McGill, S.F., Murray, B.C., Maher, K.A., Lieske, J.H.J., Rowan, L.R., 1988. Quaternary history of the Manix fault, Lake Manix basin, Mojave Desert, California. San Bernardino County Mus. Assoc. Quart. 35 (3 and 4), 3–20.
Meek, N., 1989a. Geomorphic and hydrologic implications of the rapid incision of Afton Canyon, Mojave Desert, California. Geology 17, 7–10.
Meek, N., 1989b. Physiographic history of the Afton basin, revisited. In: Reynolds, R.E. (Ed.), The West-central Mojave Desert: Quaternary Studies Between Kramer and Afton Canyon. San Bernardino County Museum Association Special Publication, pp. 78–83.
Meek, N., 1990. Late Quaternary Geochronology and Geomorphology of the Manix Basin, San Bernardino County, California. Ph.D. thesis. University of California 212 p.
Meek, N., 1994. The stratigraphy and geomorphology of Coyote basin. In: Reynolds, J. (Ed.), Calico, Coyote Basin & Lake Havasu Giants. San Bernardino County Museum Association Quarterly Vol. 41, pp. 5–13 no. 3.
Meek, N., 1999. New discoveries about the Late Wisconsinan history of the Mojave River system. In: Reynolds, R.E., Reynolds, J. (Eds.), Tracks along the Mojave: A Field Guide From Cajon Pass to the Calico Mountains and Coyote Lake. San Bernardino Museum Quarterly Vol. 46, pp. 113–117 no. 3.
Meek, N., 2000. The late Wisconsinan history of the Afton Canyon area, Mojave Desert, California. In: Reynolds, R.E., Reynolds, J. (Eds.), Empty Basins, Vanished Lakes: The Year 2000 Desert Symposium Field Guide, Volume 47, no. 2: Redlands. San Bernardino County Museum Association Quarterly, pp. 32–34.
Meek, N., 2004. Mojave River history from an upstream perspective. In: Reynolds, R.E. (Ed.), Breaking Up—The 2004 Desert Symposium Field Trip and Abstracts: Fullerton, Calif.California State University, Desert Studies Consortium, pp. 41–49
Meek, N., 2015. Evidence for middle Pleistocene surface uplift of the northern Cady Mountains, California. In: Reynolds, R.E. (Ed.), Mojave Miocene: The 2015 Desert Symposium Field Guide and Proceedings: Fullerton, Calif., California State University, Desert Studies Consortium, pp. 223–232.
Meek, N., Douglass, J., 2001. Lake overflow: an alternative hypothesis for Grand Canyon incision and development of the Colorado River. In: Young, R.A., Spamer, E.E. (Eds.), Colorado River—Origin and Evolution, Monograph Number 12. Grand Canyon Association, Grand Canyon, Arizona, pp. 199–206.
Menges, C.M., 2008. Multistage late Cenozoic evolution of the Amargosa River drainage, southwestern Nevada and eastern California. In: Reheis, M.C., Hershler, R., Miller, D. M. (Eds.), Late Cenozoic Drainage History of the Southwestern Great Basin and Lower Colorado River Region: Geologic and Biotic Perspectives: Geological Society of America Special Paper 439, Boulder, Colo., pp. 39–90
Miller, D.M., Yount, J.L., 2002. Late Cenozoic tectonic evolution of the north-central Mojave Desert inferred from fault history and physiographic evolution of the Fort Irwin area, California. Geol. Soc. Am. Mem. 195, 173–197.
Miller, D.M., Reheis, M.C., Wan, E., Wahl, D.B., Olson, H., 2011. Pliocene and early Pleistocene paleogeography of the Coyote Lake and Alvord Mountain area, Mojave Desert, California. In: Reynolds, R.E. (Ed.), The Incredible Shrinking Pliocene, California State University Desert Studies Symposium, April 2011, pp. 53–67.
Miller, D.M., Dudash, S.L., McGeehin, J.P., 2019. Paleoclimate record for Lake Coyote, California, and the last glacial maximum and deglacial paleohydrology (25–14 cal ka) of the Mojave River. In: Starratt, S.W., Rosen, M.R. (Eds.), From Saline to Freshwater: The Diversity of Western Lakes in Space and Time https://doi.org/10.1130/2018.2536(12) Special Paper 536. Geological Society of America, 20 p.
Miller, D.M., Langenheim, V.E., Haddon, E.K., 2020. Geologic map and borehole stratigraphy of Hinkley Valley and vicinity, San Bernardino County, California. U.S. Geological Survey Scientific Investigations Map 3458, 23 p., Scales 1:24,000 and 1:30,000 https://doi.org/10.3133/sim3458.
Moseley, C.G., 1978. The Geology of a Portion of the Northern Cady Mountains, Mojave Desert, California. M.S. thesis. University of California Riverside 131 p.
Nagy, E.A., Murray, B., 1996. Plio-Pleistocene deposits adjacent to the Manix fault: implications for the history of the Mojave River and transverse Ranges uplift. Sediment. Geol. 103, 9–21.
Nagy, E.A., Murray, B.C., 1991. Stratigraphy and intra-basin correlation of the Mojave River Formation, central Mojave Desert, California. In: Reynolds, R.E. (Ed.), Redlands, Calif., San Bernardino County Museum Association Quarterly. Vol. 38, pp. 5–30 No. 2.
Oviatt, C.G., 1997. Lake Bonneville fluctuations and global climate change. Geology 25, 155–158.
Oviatt, C.G., Thompson, R.S., Kaufman, D.S., Bright, J., Forester, R.M., 1999. Reinterpretation of the Burmester core, Bonneville Basin, Utah. Quat. Res. 52, 180–184.
Oviatt, C.G., Reheis, M.C., Miller, D.M., Lund, S.P., 2007. Stratigraphy of Lake Manix beds in the Manix subbasin, Mojave Desert, CA. Geol. Soc. Am. Abstr. Progr. 39 (6), 271.
Paces, J.B., Reheis, M.C., 2021. Uranium- and thorium-isotope data used to estimate uranium-series ages of Pleistocene lake deposits in the Lake Manix basin, Mojave Desert, California. U.S. Geological Survey Data Release https://doi.org/10.5066/P9MPY6R6 https://www.sciencebase.gov/catalog/item/60999058d34ea221ce33f68e.
Phillips, F.M., 2008. Geological and hydrological history of the paleo-Owens River drainage since the late Miocene. In: Reheis, M.C., Hershler, R., Miller, D.M. (Eds.), Late Cenozoic Drainage History of the Southwestern Great Basin and Lower Colorado River Region: Geologic and Biotic Perspectives. Geological Society of America Special Paper vol. 439, pp. 115–150.
Placzek, C., Quade, J., Patchett, P.J., 2006. Geochronology and stratigraphy of late Pleistocene lake cycles on the southern Bolivian Altiplano: implications for causes of tropical climate change. Geol. Soc. Am. Bull. 118, 515–532.
Pluhar, C.J., Kirschvink, J.L., Adams, R.W., 1991. Magnetostratigraphy and clockwise rotation of the Plio-Pleistocene Mojave River Formation, central Mojave Desert, California. San Bernardino County Mus. Quart. Redlands Calif. 38, 31–42.
Reheis, M., Redwine, J., Adams, K., Stine, S., Parker, K., Negrini, R., Burke, R., Kurth, G., McGeehin, J., Paces, J., Phillips, F., Sarna-Wojcicki, A., Smoot, J., 2003. Pliocene to Holocene lakes in the western Great Basin: New perspectives on paleoclimate, landscape dynamics, tectonics, and paleodistribution of aquatic species. In: Easterbrook, D.J. (Ed.), Quaternary Geology of the United States (INQUA 2003 Field Guide Volume). Desert Research Institute, Reno, pp. 155–194.
Reheis, M.C., Miller, D.M., 2010. Environments of nearshore lacustrine deposition in the Pleistocene Lake Manix basin, south-central California. In: Reynolds, R.E., Miller, D.M. (Eds.), Overboard in the Mojave: 20 Million Years of Lakes and Wetlands: Abstracts of Proceedings, 2010 Desert Symposium, Zzyzx, Calif., pp. 24–37
Reheis, M.C., Redwine, J.L., 2008. Lake Manix shorelines and Afton Canyon terraces: implications for incision of Afton Canyon. In: Reheis, M.C., Hershler, R., Miller, D.M. (Eds.), Late Cenozoic Drainage History of the Southwestern Great Basin and Lower Colorado River Region: Geologic and Biotic Perspectives. Geological Society of America Special Paper 439, pp. 227–260.
Reheis, M.C., Sowers, J.M., Taylor, E.M., McFadden, L.D., Harden, J.W., 1992. Morphology and genesis of carbonate soils on the Kyle Canyon fan, Nevada, U.S.A. Geoderma 52, 303–342.
Reheis, M.C., Sarna-Wojcicki, A.M., Reynolds, R.L., Repenning, C.A., Mifflin, M.D., 2002a. Pliocene to middle Pleistocene lakes in the western Great Basin: ages and connections. In: Hershler, R., Madsen, D.B., Currey, D.R. (Eds.), Great Basin Aquatic Systems History vol. 33. Smithsonian Institution Press, Washington, D.C., pp. 53–108.
Reheis, M.C., Stine, S., Sarna-Wojcicki, A.M., 2002b. Drainage reversals in Mono Basin during the late Pliocene and Pleistocene. Geol. Soc. Am. Bull. 114, 991–1006.
Reheis, M.C., Miller, D.M., Redwine, J.L., 2007. Quaternary stratigraphy, drainage-basin development, and geomorphology of the Lake Manix basin, Mojave Desert. U.S. Geol. Surv. Open-File Rep. 2007-1281 31 p.
Reheis, M.C., Bright, J., Lund, S.P., Miller, D.M., Skipp, G., Fleck, R.J., 2012. A half-million-year record of paleoclimate from the Lake Manix core, Mojave Desert, California. Palaeogeogr. Palaeoclimatol. Palaeoecol. 365–366, 11–37.
Reheis, M.C., Adams, K.D., Oviatt, C.G., Bacon, S.N., 2014a. Pluvial lakes in the Great Basin of the western United States—a view from the outcrop. Quat. Sci. Rev. 97, 1–25.
Reheis, M.C., Redwine, J.R., Wan, E., McGeehin, J.P., VanSistine, D.P., 2014b. Surficial geology and stratigraphy of Pleistocene Lake Manix, San Bernardino County, California. U.S. Geol. Surv. Sci. Investig. Map SIM 3312 53 p., scale 1:15,000.
Reheis, M.C., Miller, D.M., McGeehin, J.P., Redwine, J.R., Oviatt, C.G., Bright, J., 2015. Directly dated MIS 3 lake-level record from Lake Manix, Mojave Desert, California, USA. Quat. Res. 83, 187–203.
Reynolds, R.E., Reynolds, R.L., 1985. Late Pleistocene faunas from Daggett and Yermo, San Bernardino County, California. In: Reynolds, R.E. (Ed.), Cajon Pass to Manix Lake: Geological investigations along Interstate 15. San Bernardino County Museum Association Special Publication, pp. 175–191.
Rosenbaum, J.G., Kaufman, D.S., 2009. Paleoenvironments of Bear Lake, Utah and Idaho, and its catchment. Geol. Soc. Am. Spec. Pap. 450 351 p.
Rosenbaum, J.G., Reynolds, R.L., 2004. Record of late Pleistocene glaciation and deglaciation in the southern Cascade Range: II. Flux of glacial flour in a sediment core from Upper Klamath Lake, Oregon. J. Paleolimnol. 31, 235–252.
Rossman, P.I.I., Howard, A.D., 2002. Drainage basin evolution in Noachian Terra Cimmeria. Mars: J. Geophys. Res. 107, 23.
Sack, D., 2002. Fluvial linkages in Lake Bonneville subbasin integration. In: Hershler, R., Madsen, D.B., Currey, D.R. (Eds.), Great Basin Aquatic Systems History. vol. 33. Smithsonian Institution Press, Washington, D.C., pp. 129–144.
Sadler, P.M., 1981. Sediment accumulation rates and the completeness of stratigraphic sections. J. Geol. 89, 569–584.
Sarna-Wojcicki, A.M., Bowman, H.R., Meyer, C.E., Russell, P.C., Woodward, M.J., McCoy, G., Rowe Jr., J.J., Baedecker, P.A., Asaro, F., Michael, H., 1984. Chemical analyses, correlations, and ages of upper Pliocene and Pleistocene ash layers of east-central and southern, California. U.S. Geol. Surv. Prof. Paper 1293 40 p.
Shanmugam, G., 2016. The seismite problem. J. Palaeogeogr. 5, 318–362. https://doi.org/10.1016/j.jop.2016.06.002.

Smith, G.I., Barczak, V.J., Moulton, G., Liddicoat, J.C., 1983. Core KM-3, a surface to bedrock record of late Cenozoic sedimentation in Searles Valley, California. U.S. Geol. Surv. Prof. Paper 1256 24 p.

Smith, G.I., Bischoff, J.L., Bradbury, J.P., 1997. Synthesis of the paleoclimatic record from Owens Lake core OL-92. In: Smith, G.I., Bischoff, J.L. (Eds.), An 800,000-Year Paleoclimatic Record from Core OL-92, Owens Lake, Southeast California. Geological Society of America Special Paper vol. 317, pp. 143–160.

Smith, G.R., Dowling, T.E., Gobalet, K.W., Lugaski, T., Shiozawa, D.K., Evans, R.P., 2002. Biogeography and timing of evolutionary events among Great Basin fishes. In: Hershler, R., Madsen, D.B., Currey, D.R. (Eds.), Great Basin Aquatic Systems History. Vol. 33. Smithsonian Institution Press, Washington, DC, pp. 175–234.

Steiger, R.H., Jäger, E., 1977. Subcommission on geochronology: convention on the use of decayconstants in geo- and cosmochronology. Earth Planet. Sci. Lett. 36, 359–362. https://doi.org/10.1016/0012-821X(77)90060-7.

Steinmetz, J.J., 1987. Ostracodes from the late Pleistocene Manix Formation, San Bernardino County, California. In: Reynolds, J. (Ed.), Quaternary History of the Mojave Desert. San Bernardino, San Bernardino County Museum Association Quarterly Vol. 34, pp. 46–47 nos. 3 and 4.

Steinmetz, J.J., 1988. Biostratigraphy and Paleoecology of Limnic Ostracodes From the Late Pleistocene Manix Formation. M.S. thesis. California State Polytechnic University, Pomona.

Unruh, J.R., Lettis, W.R., Sowers, J.M., 1994. Kinematic interpretation of the 1992 Landers earthquake. Bull. Seismol. Soc. Am. 84, 537–546 (scale 1:48,000).

Wehmiller, J.F., Miller, G.H., 2000. Aminostratigraphic dating methods in Quaternary geology. In: Noller, J.S., Sowers, J.M., Letis, W.R. (Eds.), Quaternary Geochronology: Methods and Applications, American Geophysical Union Reference Shelf. 4, pp. 187–222.

Wells, S.G., Brown, W.J., Enzel, Y., Anderson, R.Y., McFadden, L.D., 2003. Late Quaternary geology and paleohydrology of pluvial Lake Mojave, southern California. In: Enzel, Y., Wells, S.G., Lancaster, N. (Eds.), Paleoenvironments and Paleohydrology of the Mojave and Southern Great Basin Deserts: Boulder, Colo. Geological Society of America Special Paper 368, pp. 79–114.